Time Calibrated Morpho-molecular Classification of Nassellaria (Radiolaria)

Miguel M Sandin, Loïc Pillet, Tristan Biard, Camille Poirier, Estelle Bigeard, Sarah Romac, Noritoshi Suzuki, Fabrice Not

Protist, Vol. 170, 187–208, April 2019
http://www.elsevier.de/protis
Published online date 22 February 2019

Protist

ORIGINAL PAPER

Time Calibrated Morpho-molecular Classification of Nassellaria (Radiolaria)

Miguel M. Sandin[a,1], Loïc Pillet[a], Tristan Biard[a], Camille Poirier[a], Estelle Bigeard[a], Sarah Romac[a], Noritoshi Suzuki[b], and Fabrice Not[a]

[a]Sorbonne Université, CNRS – UMR7144 – Ecology of Marine Plankton Group – Station Biologique de Roscoff, 29680 Roscoff, France
[b]Department of Earth Science, Graduate School of Science, Tohoku University, Sendai 980-8578, Japan

Submitted October 3, 2018; Accepted February 7, 2019
Monitoring Editor: David Moreira

Nassellaria are marine protists belonging to the Radiolaria lineage (Rhizaria). Their skeleton, made of opaline silica, exhibit an excellent fossil record, extremely valuable in micro-paleontological studies for paleo-environmental reconstruction. Yet, to date very little is known about the extant diversity and ecology of Nassellaria in contemporary oceans, and most of it is inferred from their fossil record. Here we present an integrative classification of Nassellaria based on taxonomical marker genes (18S and 28S ribosomal DNA) and morphological characteristics obtained by optical and scanning electron microscopy imaging. Our phylogenetic analyses distinguished 11 main morpho-molecular clades relying essentially on the overall morphology of the skeleton and not on internal structures as previously considered. Using fossil calibrated molecular clock we estimated the origin of Nassellaria among radiolarians primitive forms in the Devonian (ca. 420 Ma), that gave rise to living nassellarian groups in the Triassic (ca. 250 Ma), during the biggest diversification event over their evolutionary history. This morpho-molecular framework provides both a new morphological classification easier to identify under light microscopy and the basis for future molecular ecology surveys. Altogether, it brings a new standpoint to improve our scarce understanding of the ecology and worldwide distribution of extant nassellarians.

Key words: Nasselaria; calibrated molecular clock; morpho-molecular classification; rDNA; silica skeleton; ecology.

Introduction

Along with Foraminifera, Radiolaria constitute the Phylum Retaria, within the supergroup Rhizaria, one of the 8 major branches of eukaryotic life (Burki and Keeling 2014). Radiolarians are marine heterotrophic protists, currently classified in 5 taxonomic orders based on morphological features and chemical composition of their biomineralized skeleton. Acantharia possess a skeleton made out of strontium sulfate ($SrSO_4$), while opaline silica (SiO_2 nH_2O) is found in skeletons of Taxopodia and the polycystines Collodaria, Nassellaria and Spumellaria (Suzuki and Not 2015). The robust silica skeleton of polycystines preserves well in

[1]Corresponding author.
e-mail miguelmendezsandin@gmail.com (M.M. Sandin).

https://doi.org/10.1016/j.protis.2019.02.002

sediments and hard sedimentary rocks, providing an extensive fossil record throughout the Phanerozoic (De Wever et al. 2001). Essentially studied by micro-palaeontologists, classification and evolutionary history of Radiolaria are largely based on morphological criteria (Suzuki and Oba 2015) and very little is known about the ecology and diversity of contemporary species.

Among polycystines, Nassellaria actively feed on a large variety of prey, from bacteria to mollusc larvae (Anderson et al. 1993; Sugiyama et al. 2008), contributing significantly to trophic webs dynamic of oceanic ecosystems. Some nassellarian species host photosynthetic algal symbionts, up to 50 symbionts per host cells, mainly identified as dinoflagellates (Decelle et al. 2015; Probert et al. 2014; Suzuki and Not 2015; Zhang et al. 2018). This mixotrophic behaviour may influence their distribution patterns, being in surface tropical waters the greatest diversity and abundance values, and decreasing towards the poles and at depth (Boltovskoy and Correa 2016; Boltovskoy 2017). Only a few taxa are restricted to deep waters (1000–3000 m) in which no photosymbionts have ever been described (Suzuki and Not 2015).

Unlike other radiolarians, the nassellarian skeleton is heteropolar, aligned along an axis and not a centre. This skeleton is divided in three main different segments: the cephalis always present (or 1st segment), the thorax (2nd segment) and sometimes an abdomen (3rd segment) and post-abdominal segments (Campbell 1954). The cephalis contains the initial spicular system, whose structure was widely used for the taxonomic classification at family or higher levels due to its early development in the ontogenetic growth (De Wever et al. 2001; Petrushevskaya 1971b). Its basic architecture is the component of *A*-rod (apical rod), *D*- (dorsal rod), *V*- (ventral rod), *MB* (median bar), occasionally Ax (axobate node), *l*-rod (lateral rod from *MB* at the *A*-rod side) and *L*-rod (lateral rod from *MB* at the *V*-rod side). All these initial spicules except for *V*- and *l*-rods are always present in Nassellaria (Supplementary Material Fig. S1). The architecture of the initial spicular system has been used not only in nassellarian classification but also for Collodaria, Spumellaria and other Polycystines such as Entactinaria, a group considered to be an early lineage in the Paleozoic. Morphology-based taxonomic classifications have divided extant Nassellaria into nearly 25 families, 140 genera and 430 recognized species (Suzuki and Not 2015). At higher level, they are currently divided into 7 super-families: Acanthodesmoidea (sensu Dumitrica in De Wever et al. 2001; Hertwig 1879), Acropyramioidea (Haeckel 1882; sensu emend. Petrushevskaya 1981), Artostrobioidea (sensu O'Dogherty 1994; Riedel 1967), Cannobotryoidea (Haeckel 1882; sensu Petrushevskaya 1971a), Eucyrtidioidea (sensu Dumitrica in De Wever et al. 2001; Ehrenberg 1846), Plagiacanthoidea (Hertwig 1879; sensu Petrushevskaya 1971a), Pterocorythoidea (Haeckel 1882; sensu Matsuzaki et al. 2015) and some undetermined families (i.e., Theopiliidae, Bekomidae, Carpocaniidae) (Matsuzaki et al. 2015).

The expertise required to collect, sort and identify living nassellarian specimens along with their short maintenance time in cultures (Anderson et al. 1989; Suzuki and Not 2015) make the study of their taxonomy and ecology arduous. In addition, the low DNA concentration per individual cell challenges the molecular approach to address such questions. Phylogenetic studies have demonstrated the effectiveness of combining single cell DNA sequencing and imaging data in assessing classification and evolutionary issues beyond morphological characteristics (Bachy et al. 2012; Biard et al. 2015; Decelle et al. 2012b). Acquisition of reference DNA barcode based on single cell sequencing of isolated specimens have also established the basis for further molecular ecology surveys inferring the actual diversity and ecology in the nowadays oceans (Biard et al. 2017; Decelle et al. 2013; Nitsche et al. 2016). In addition, the use of fossil-calibrated molecular clock has become a popular tool in molecular evolution, addressing diversification rates (e.g., in diatoms; Lewitus et al. 2018), exploring co-evolution processes (e.g., Acantharia and *Phaeocystis*; Decelle et al. 2012a; or bees and eudicots; Cardinal and Danforth 2013), resolving evolutionary patterns along with the fossil record (e.g., on Ray finned fishes; Giles et al. 2017; or in holothuroids; Miller et al. 2017) or tracing the origin and the evolutionary history outside fossil limits (e.g., on the origin of eukaryotes; Douzery et al. 2004; Berney and Pawlowski 2006; Eme et al. 2014). To date, few phylogenetic studies have explored the extant genetic diversity of Nassellaria and the relationships among families and their evolutionary patterns remains still elusive (Krabberød et al. 2011; Kunitomo et al. 2006; Yuasa et al. 2009). So far, with a total of 16 sequences from morphologically described specimens, covering 5 of the 7 super-families identified, Eucyrtidioidea was considered as the most basal and the rest of the represented groups have uncertain phylogenetic positions (Krabberød et al. 2011).

The latest classification of Nassellaria (Matsuzaki et al. 2015) attempted to integrate

the extensive morphological knowledge (De Wever et al. 2001; Haeckel 1882; Hertwig 1879; Petrushevskaya 1971a;) with the few molecular analyses performed for Nassellaria (Krabberød et al. 2011). Here we introduce an integrative morpho-molecular classification of Nassellaria obtained by ribosomal DNA taxonomic marker genes (18S and partial 28S rDNA) and imaging techniques (light microscopy, scanning electron microscopy and/or confocal microscopy), compared with the current morphological classification. In addition, the extensive fossil record available for Nassellaria allowed us to time-calibrate our phylogenetic analysis based on molecular dating and infer their evolutionary history contextualized with geological environmental changes at a global scale. Finally, the inclusion of environmental sequences gave insights in the extant genetic diversity of nassellarians in contemporary oceans.

Results

Comparative Molecular Phylogeny and Morphological Taxonomy

The final molecular phylogeny is composed of 90 distinct nassellarian specimens generated by 61 sequences of the 18S rDNA gene and of 57 sequences of the partial 28S (D1 and D2 regions) rDNA gene (Supplementary Material Table S2). From the 61 final sequences of the 18S rDNA gene, 38 were obtained in this study and 23 were previously available, of which 16 have been morphologically identified and 7 are environmental. Regarding the partial 28S rDNA gene, 55 new sequences were obtained in this study and 2 were previously available and morphologically described. The final alignment matrix has 32.4% of invariant sites, and in total includes 67 new sequences. All of these specimens cover 7 superfamilies (Acanthodesmoidea, Acropyramioidea, Artostrobioidea, Cannobotryoidea, Eucyrtidioidea, Plagiacanthoidea, Pterocorythoidea, and three undefined families), based on morphological observations performed with light microscopy (LM; Supplementary Material Fig. S3), scanning electron microscopy (SEM) and/or confocal microscopy (CM) on the exact same specimens for which we obtain a sequence. Overall, molecular phylogeny is consistent with morphological classification at the superfamily level, although there are some specific discrepancies. The phylogenetic analysis shows 11 clades (Fig. 1) clearly differentiated with high values of ML bootstrap (BS > 99) and posterior probabilities (PP > 0.86).

Clade A holds the most basal position with 16 sequences of which 10 are novel sequences, 5 were previously available and one is environmental. All specimens clustering within this clade (Figs 2A, 3A) have a simple and round cephalis, an apical horn, a small ventral rod and multisegmented (cephalis, thorax and several abdomen) skeleton with distinctive inner rings, that correspond to the Superfamily Eucyrtidioidea. All multisegmented nassellarians with spherical cephalis encountered in our study belong to this superfamily, both morphologically and phylogenetically. The rest of the clades group together with a high BS (100) and PP (1) values. Thereafter clades B, C, D and E cluster together in lineage II. Clades X, F and G constitute the lineage III, highly supported (100 BS and 1 PP) as sister group of the lineage IV. This last lineage it is composed by the clades H, as the basal group and clades I and J highly related phylogenetically (100 BS and 1 PP).

Within lineage II, clade B is represented by only one sequence from this study (Osh128), and its morphology matches with the superfamily Acropyramioidea (Figs 2B, 3B) exhibiting a pyramidal skeleton constituted of a reduced cephalis and thorax. Clade C is composed by two novel sequences (Figs 2C, 3C). Their overall round morphology and a characteristic small and flat cephalis not well distinguished from the thorax agrees with the undetermined family Carpocaniidae (De Wever et al. 2001; Petrushevskaya 1971a). Its sister clade, the Clade D is constituted by three new (Ses58, Mge17-70 and Mge17-9) and one environmental sequences, and the morphology of these specimens (Figs 2D, 3D) agrees with the definition of the Superfamily Artostrobioidea. They share a multisegmented skeleton without significant inner rings, a hemispherical cephalis and an important ventral rod. The last clade of the lineage II, clade E, gathers four new sequences, one and two environmental sequences. This clade includes all the monocyrtid (cephalis) nassellarians where the spines A and V are merged forming the so-called D-ring (Acanthodesmoidea). There are representatives for two out of three families (Stephaniidae is the missing family), yet no phylogenetic differences were found for the included families, Acanthodesmiidae (Figs 2E1, 3E1) and Triospyrididae (Figs 2E2-E4, 3E2).

In lineage III, clades X and F are highly supported as sister clades (100 BS and 1 PP). Clade X is established by two novel sequences morphologically identified as *Archipilium johannismonicae* (Figs 2X1, 3X1) and *Enneaphormis enneastrum*

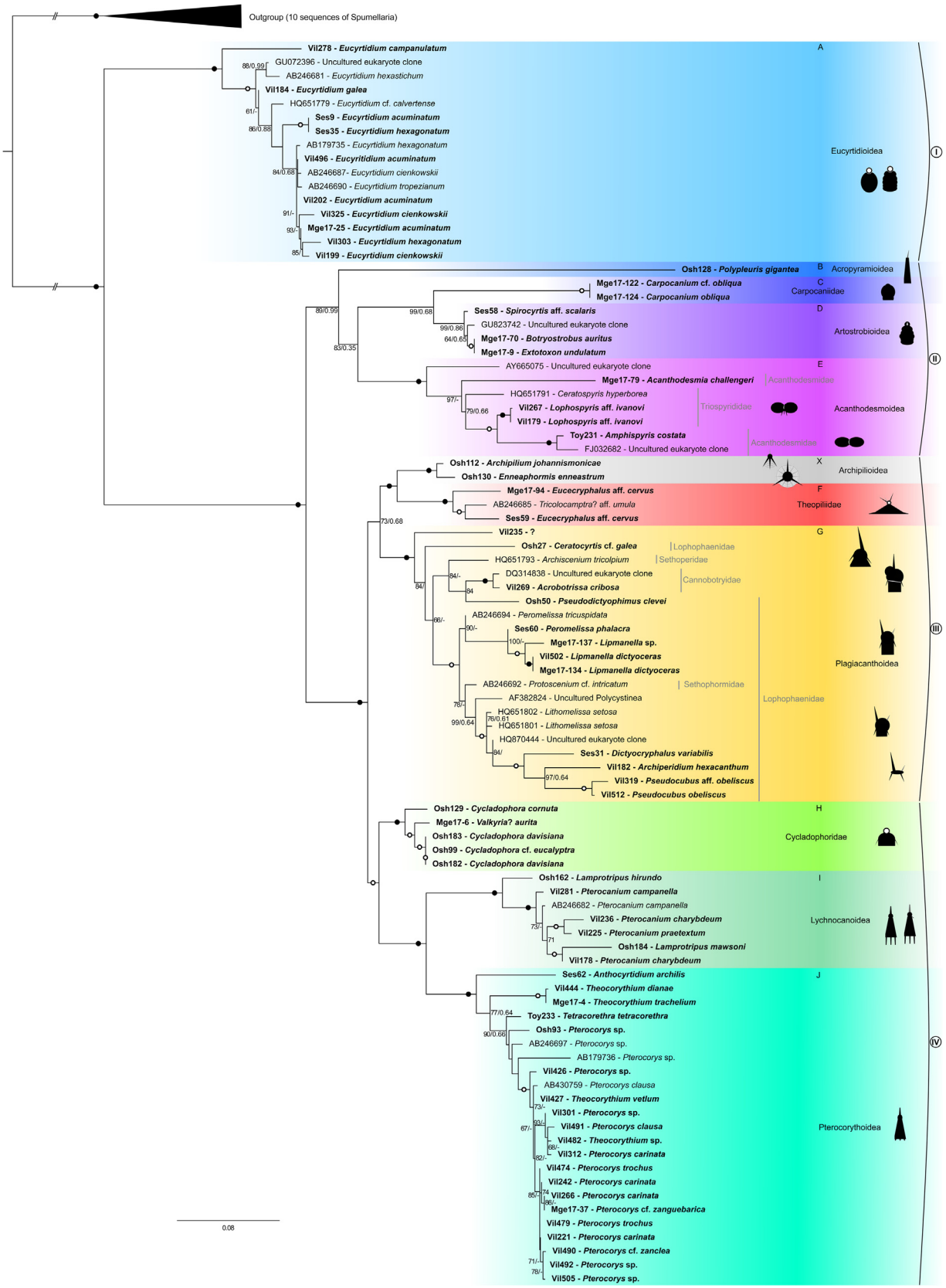
Outgroup (10 sequences of Spumellaria)
Vil278 - Eucyrtidium campanulatum
GU072396 - Uncultured eukaryote clone
AB246681 - Eucyrtidium hexastichum
Vil184 - Eucyrtidium galea
HQ651779 - Eucyrtidium cf. calvertense
Ses9 - Eucyrtidium acuminatum
Ses35 - Eucyrtidium hexagonatum
AB179735 - Eucyrtidium hexagonatum
Vil496 - Eucyritidium acuminatum
AB246687- Eucyrtidium cienkowskii
AB246690 - Eucyrtidium tropezianum
Vil202 - Eucyrtidium acuminatum
Vil325 - Eucyrtidium cienkowskii
Mge17-25 - Eucyrtidium acuminatum
Vil303 - Eucyrtidium hexagonatum
Vil199 - Eucyrtidium cienkowskii
A
Eucyrtidioidea
I
Osh128 - Polypleuris gigantea
B
Acropyramioidea
Mge17-122 - Carpocanium cf. obliqua
Mge17-124 - Carpocanium obliqua
C
Carpocaniidae
Ses58 - Spirocyrtis aff. scalaris
GU823742 - Uncultured eukaryote clone
Mge17-70 - Botryostrobus auritus
Mge17-9 - Extotoxon undulatum
D
Artostrobioidea
II
AY665075 - Uncultured eukaryote clone
Mge17-79 - Acanthodesmia challengeri
Acanthodesmidae
HQ651791 - Ceratospyris hyperborea
Triospyridinidae
Vil267 - Lophospyris aff. ivanovi
Vil179 - Lophospyris aff. ivanovi
Toy231 - Amphispyris costata
FJ032682 - Uncultured eukaryote clone
Acanthodesmidae
E
Acanthodesmoidea
Osh112 - Archipilium johannismonicae
Osh130 - Enneaphormis enneastrum
X
Archipilioidea
Mge17-94 - Eucecryphalus aff. cervus
AB246685 - Tricolocamptra? aff. umula
Ses59 - Eucecryphalus aff. cervus
F
Theopiliidae
Vil235 - ?
Osh27 - Ceratocyrtis cf. galea
Lophophaenidae
HQ651793 - Archiscenium tricolpium
Sethoperidae
DQ314838 - Uncultured eukaryote clone
Vil269 - Acrobotrissa cribosa
Cannobotryidae
Osh50 - Pseudodictyophimus clevei
AB246694 - Peromelissa tricuspidata
Ses60 - Peromelissa phalacra
Mge17-137 - Lipmanella sp.
Vil502 - Lipmanella dictyoceras
Mge17-134 - Lipmanella dictyoceras
G
III
Plagiacanthoidea
AB246692 - Protoscenium cf. intricatum
Sethophormidae
AF382824 - Uncultured Polycystinea
HQ651802 - Lithomelissa setosa
HQ651801 - Lithomelissa setosa
HQ870444 - Uncultured eukaryote clone
Ses31 - Dictyocryphalus variabilis
Vil182 - Archiperidium hexacanthum
Vil319 - Pseudocubus aff. obeliscus
Vil512 - Pseudocubus obeliscus
Lophophaenidae
Osh129 - Cycladophora cornuta
Mge17-6 - Valkyria? aurita
Osh183 - Cycladophora davisiana
Osh99 - Cycladophora cf. eucalyptra
Osh182 - Cycladophora davisiana
H
Cycladophoridae
Osh162 - Lamprotripus hirundo
Vil281 - Pterocanium campanella
AB246682 - Pterocanium campanella
Vil236 - Pterocanium charybdeum
Vil225 - Pterocanium praetextum
Osh184 - Lamprotripus mawsoni
Vil178 - Pterocanium charybdeum
I
Lychnocanoidea
Ses62 - Anthocyrtidium archilis
Vil444 - Theocorythium dianae
Mge17-4 - Theocorythium trachelium
Toy233 - Tetracorethra tetracorethra
Osh93 - Pterocorys sp.
AB246697 - Pterocorys sp.
AB179736 - Pterocorys sp.
Vil426 - Pterocorys sp.
AB430759 - Pterocorys clausa
Vil427 - Theocorythium vetlum
Vil301 - Pterocorys sp.
Vil491 - Pterocorys clausa
Vil482 - Theocorythium sp.
Vil312 - Pterocorys carinata
Vil474 - Pterocorys trochus
Vil242 - Pterocorys carinata
Vil266 - Pterocorys carinata
Mge17-37 - Pterocorys cf. zanguebarica
Vil479 - Pterocorys trochus
Vil221 - Pterocorys carinata
Vil490 - Pterocorys cf. zanclea
Vil492 - Pterocorys sp.
Vil505 - Pterocorys sp.
J
IV
Pterocorythoidea
0.08

(Figs. 2X2, 3X2). These two specimens have a very short or missing median bar (MB) allowing the development of three large feet with a three-pointed star (dorsal and lateral, left and right, rays) shape forming a significant circular frame where they build the thorax when present. In Clade F there are two novel sequences (Ses59 and Mge17-94) and a previously available sequence. These specimens are morphologically identified in the genus *Eucecryphalus* (Figs 2F, 3F) and a third specimen as *Tricolocamptra* (AB246685). The former genus belongs to the undetermined family Theopiliidae (De Wever et al. 2001; Matsuzaki et al. 2015) with a hat shaped morphology and pronounced segmentation. The genus *Eucecryphalus*, the senior synonym of *Theopilium*, is the type genus of the family Theopiliidae (Matsuzaki et al. 2015), and thus Clade F is automatically specified as the "true" Theopiliidae. The taxonomic position of the second genus, *Tricolocamptra*, varies through references and the available image for the specimen lacks taxonomical resolution, therefore it is not possible to establish the link with any described morphological group.

With 14 different morpho-species and 11 different genus, Clade G is the most morphologically diverse clade. While all specimens have consistently one or two segments, the complexity of the cephalis and the sizes of the rays vary widely (Figs 2G1-G6, 3G2-G6). Specimen HQ651793 (*Archiscenium tricolpium*) corresponds to the Family Sethophormidae (Sethophormidae Haeckel 1882, sensu emend. Petrushevskaya 1971a) within the Superfamily Plagiacanthoidea. The large cephalis and the umbrella shape of the thorax are characteristics of this family. The specimen Vil269 (Figs 2G3, 3G3, *Acrobotrissa cribosa*) agrees with the description of the Superfamily Cannobotryoidea and its complex cephalic structure subdivided in different lobes is the main characteristic. The rest of the specimens of clade G can be grouped within the Family Lophophaenidae (Lophophaenidae Haeckel, 1882, *sensu* Petrushevskaya, 1971a), still within Plagiacanthoidea. Within this family there are two different subclades, those specimens with a prominent thorax (e.g. Mge17-134, *Lipmanella dictyoceras*, Fig. 2G4; Mge17-137, *Lipmanella* sp. Fig. 3G4) and those with a barely defined thorax (e.g., Ses60, *Peromelissa phalacra,* Figs 2G5, 3G5) or not-defined thorax (e.g. Vil512, *Pseudocubus obeliscus*, Figs 2G6, 3G6). Two last specimens, Osh27 (*Ceratocyrtis* cf. *galea*, Fig. 2G1) and Osh50 (*Pseudodictyophimus clevei*; Figs 2G2, 3G2), are morphologically identified as Lophophaenidae (HQ651793: De Wever et al. 2001; and Osh50: Matsuzaki et al. 2015; Petrushevskaya 1971b) despite their phylogenetic position closely related to the Superfamily Cannobotryoidea.

Lineage IV is the most distal regarding the root of the tree. Within it, clade H is constituted by six new sequences very closely related to each other (BS > 96 and PP > 0.99). These specimens are morphologically assigned to the genus *Cycladophora* (Figs 2H1, 3H) and *Valkyria* (Fig. 2H2). Specimens from clade H show a conical and campanulate shaped morphology with a distinguishable cephalis and an apical horn compared to the wide thorax and not distinguished cephalis with two (V and A) rods of *Eucecryphalus*. Clade I is composed of six novel sequences and one previously available, while clade J gathers twenty new sequences and 3 previously available. These clades comprise nassellarians with an apical stout horn, a spherical (clade I) or elongated cephalis (clade J) and a truncated conical thorax; the abdomen, if present, is also truncated and sometimes not well defined, agreeing with the definition of the Superfamily Pterocorythoidea. Clade J corresponds to those with elongated cephalis (Figs 2J, 3J) or Pterocorythidae (Pterocorythidae Haeckel, 1882, sensu De Wever et al. 2001). Clade I includes nassellarians with spherical head, ventral short ray and three feet (Figs 2I2, 3.I2), all characteristics of the Family Lychnocanidae (Lychnocaniidae Haeckel, 1882, sensu emend. Suzuki in Matsuzaki et al. 2015). Two specimens (Figs 2I1, 3I1) of the undetermined family Bekomidae

Figure 1. Molecular phylogeny of Nassellaria inferred from the concatenated complete 18S and partial 28S (D1-D2 regions) rDNA genes (90 taxa and 2590 aligned positions). The tree was obtained by using a phylogenetic Maximum likelihood method implemented using the GTR + γ + I model of sequence evolution. PhyML bootstrap values (100 000 replicates, BS) and posterior probabilities (PP) are shown at the nodes (BS/PP). Black circles indicate BS of 100% and PP > 0.99. Hollow circles indicates BS > 90% and PP > 0.90. Sequences obtained in this study are shown in bold. Eleven main clades are defined based on statistical support and morphological criteria (A, B, C, D, E, X, F, G, H, I, J). Figures besides clade names represent main features in the overall morphology of specimens included in the phylogeny. Ten Spumellaria sequences were assembled as outgroup. Branches with a double barred symbol are fourfold reduced for clarity.

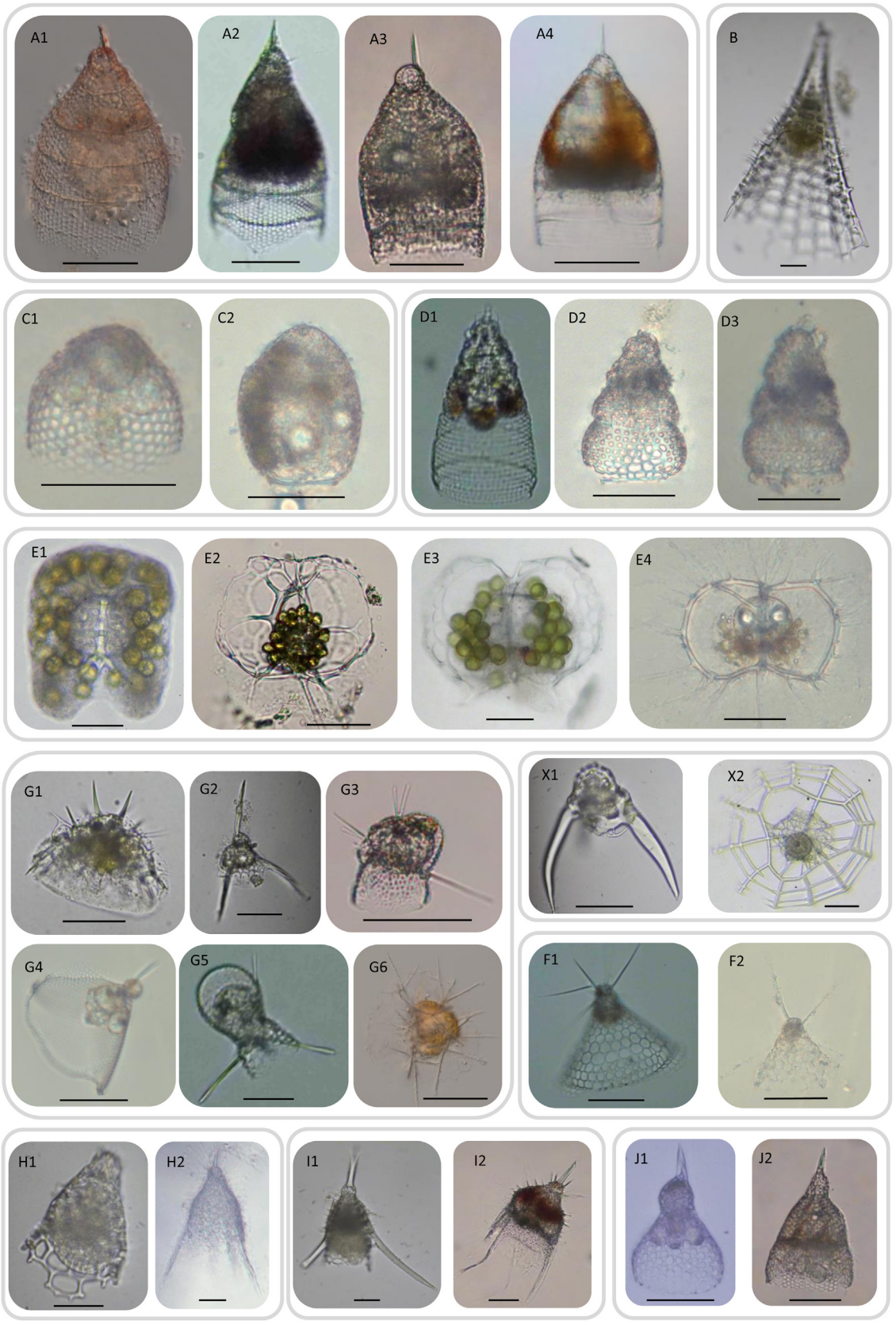
A1
A2
A3
A4
B
C1
C2
D1
D2
D3
E1
E2
E3
E4
G1
G2
G3
X1
X2
G4
G5
G6
F1
F2
H1
H2
I1
I2
J1
J2

(Bekomidae Dumitrica in De Wever et al. 2001), are scattered among clade I showing no phylogenetic differences between members of both families. The BS (93) and the PP (0.99) values establish a strong phylogenetic relationship within this lineage, and so does the overall skeleton shape.

Molecular Dating

The molecular clock dated the diversification between Spumellaria and Nassellaria (the root of the tree) with a median value of 512 Ma (95% Highest Posterior Density –HPD-: between 600 and 426 Ma) (Fig. 4). From now on, all dates are expressed as median values followed by the 95% HPD interval. Despite the large uniform distribution given to the ingroup (U [180,500]), the first diversification of Nassellaria was settled at 423 (500-342) Ma. Clade A had its first radiation dated in 245 (264-225) Ma. The common ancestor to all the other clades diversified at around 340 (419-271) Ma into two main groups, the so-called lineage II and the lineages III–IV splitting into two other lineages soon afterwards. Within lineage II, the first diversification occurs at 276 (354-209) Ma, and clades C and D diversified 197 (250-160) Ma. Thereafter in this lineage the phylogenetic relationships are dubious, however clade D diversified from any other clade 248 (315-191) Ma. Diversification within these clades was 28 (49-4) Ma for clade C, 175 (194-155) Ma for clade D and 77 (95-60) Ma for clade E. The lineages III and IV diversified from each other 274 (344-215) Ma. Lineage III rapidly diversified 243 (304-197) Ma when clades F and X split from clade G, followed by the fast diversification of clade G 196 (241-170) Ma. It was 168 (243-76) Ma when clade F separate of clade X, and 86 (157-32) Ma and 40 (106- 4) Ma when they respectively diversified. The last lineage (IV) diversified between clades H, I and J 206 (287-129) Ma, and clades I and J 138 (206-88) Ma. Despite this early divergence between clades, radiation within clades was more recent, being 87 (171-26) Ma, 70 (87-53) Ma and 73 (90-58) Ma for clades H, I and J, respectively.

Post-hoc Analyses

The lineages through time analysis (Fig. 5) shows a classic exponential diversification slope, with a 0.0109 rate of speciation (Ln(lineages)·million years^{-1}). The first diversification of extant Nassellaria (~423 Ma) corresponds to the divergence between clade A and the rest of the clades. However, the first increase in the slope (up to: 0.017, t-test: $p < 0.001$) occurs at ~275 Ma, when the main lineages start expanding; lineage II splits between clade B and clades C, D and E, clade A diversifies and the evolutionary lineages III and IV diverged from each other followed by the rapid diversification of lineage III. After this sudden increase of the main lineages, a second diversification event happened (ca. 198 Ma) where both the evolutionary lineage IV and the clade G diversify and clade C splits from clade D. Thereafter, the diversification seems to be stepped and separate in different periods of time, were only lineage III keep diversifying. The last and relatively uninterrupted diversification occurred ~82 Ma corresponding to the speciation within the already present clades and the first diversification of the clades H, F, E, J, I, X and C.

The ancestral state reconstruction analyses (Fig. 6) establish that the common ancestor to all living Nassellaria should be either multicyrtid or dicyrtid, with 1st or 2nd cephalic state (Table 2), a small apical horn, with a small or not projecting ventral ray and not projecting dorsal and lateral rays out of the skeleton. Soon after the diversification between clade A and the rest of the clades, the analysis establishes for the common ancestor

Figure 2. Light Microscopy (LM) images of live Nassellarian specimens used in this study for phylogenetic analysis. Letters correspond to its phylogenetic clade in Fig. 1. Scale bars (when available) = 50 μm. (A1) Vil496: *Eucyrtidium acuminatum*. (A2) Ses35: *Eucyrtidium hexagonatum*. (A3) Vil278: *Eucyrtidium campanulatum*. (A4) Vil184: *Eucyrtidium galea*. (B) Osh128: *Polypleuris gigantea*. (C1) Mge17-122: *Carpocanium* cf. *obliqua*. (C2) Mge17-124: *Carpocanium obliqua*. (D1) Ses58: *Spirocyrtis* aff. *scalaris*. (D2) Mge17-9: *Extotoxon undulatum*. (D3) Mge17-70: *Botryostrobus auritus*. (E1) Toy231: *Amphispyris costata*. (E2) Vil267: *Lophospyris* aff. *ivanovi*. (E3) Vil179: *Lophospyris* aff. *ivanovi*. (E4) Mge17-79: *Acanthodesmia challengeri*. (X1) Osh112: *Archipilium johannismonicae*. (X2) Osh130: *Enneaphormis enneastrum*. (F1) Ses59: *Eucecryphalus* aff. *cervus*. (F2) Mge17-94: *Eucecryphalus* aff. *cervus*. (G1) Osh27: *Ceratocyrtis* cf. *galea*. (G2) Osh50: *Pseudodictyophimus clevei*. (G3) Vil269: *Acrobotrissa cribosa*. (G4) Mge17-134: *Lipmanella dictyoceras*. (G5) Ses60: *Peromelissa phalacra*. (G6) Vil512: *Pseudocubus obeliscus*. (H1) Osh129: *Cycladophora cornuta*. (H2) Mge17-6: *Valkyria*? *aurita*. (I1) Osh162: *Lamprotripus hirundo*. (I2) Vil225: *Pterocanium praetextum*. (J1) Vil444: *Theocorythium dianae*. (J2) Vil312: *Pterocorys carinata*.

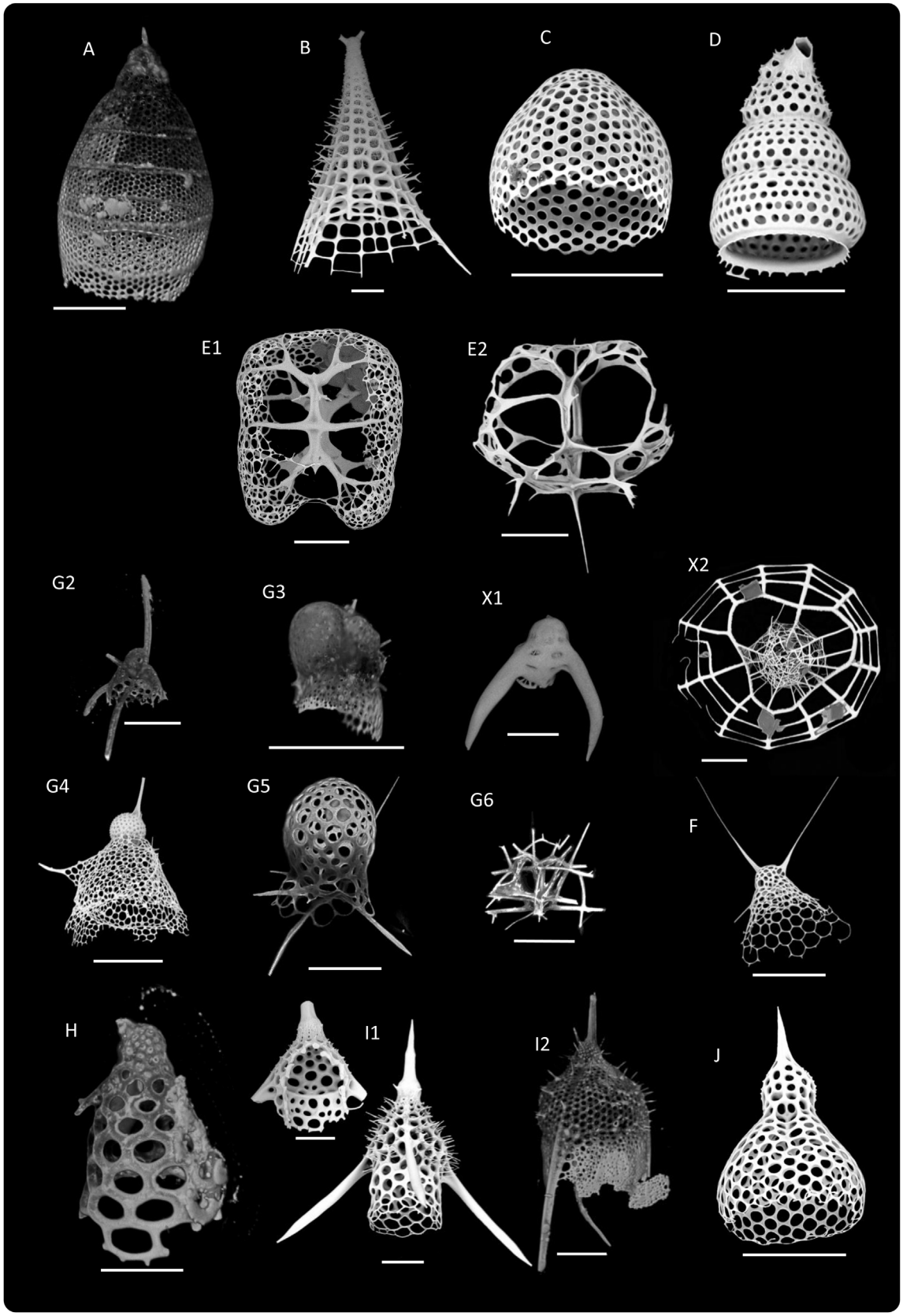
A
B
C
D
E1
E2
G2
G3
X1
X2
G4
G5
G6
F
H
I1
I2
J

of lineages II, III and IV, a dicyrtid state, with a 2nd cephalic state (Table 2), a small apical horn, and not projecting ventral, dorsal and lateral rays. The same morphology was found for the common ancestor of the lineage II, for that of lineages III and IV and that of lineage III. The dicyrtid state remains the most parsimonious state for the common ancestor of all families except for clades A and D and E. The cephalis has a 2nd state (Table 2) for every common ancestor of each clade except for clade A (1st state; Table 2), F (1st or 2nd; Table 2) and I-J (2nd or 3rd; Table 2). Regarding states of the apical ray, it remained small in every node with the exception of lineage IV, where it is medium/big. The ventral ray remained inside the skeleton with the exception of clade A, D, G and I, where it is small. Finally, the dorsal and lateral rays remained inside the skeleton for the common ancestor of clades A, B, C, D and F, but quite different states for the common ancestor of the rest of the clades: clade E has either a not projecting or small dorsal and lateral rays, clade X is characterized by big/feet/wings, clade G has a small dorsal and lateral rays, clades H and J either not projecting out of the skeleton, small or medium dorsal and lateral rays and clade I has a big/feet/wings dorsal and lateral rays.

Environmental Genetic Diversity of Nassellaria

A total of 229 18S rDNA and two 28S rDNA environmental sequences affiliated to Nassellaria were retrieved from public database and placed in our reference phylogenetic tree (Fig. 7; Supplementary Material Table S3). Most of the environmental sequences (151) belonged to clade G, while 41 other sequences were scattered between clades A, D, E, F, I and J (2, 6, 26, 1, 2 and 4 sequences respectively). The rest of the sequences could not be placed within any existing clade. From those, 28 were closely related to clade E, and the others at basal nodes mainly over lineage II. These 37 sequences were then included in a phylogenetic tree (with a GTR + G + I model, 4 invariant sites and 1000 bootstraps) and 3 new and highly supported clades appeared (Supplementary Material Fig. S2). The first clade, constituted by 31 sequences, was assigned to Collodaria in Biard et al. (2015). A second clade formed by 2 sequences (BS: 94) was highly related to clades B and C (BS: 96). And the last clade, constituted as well of 2 sequences (BS: 100) was basal to the node formed by clades C, D and the previous mentioned environmental clade (BS: 58). The 2 remaining sequences were highly related to clades I (BS: 84) and to the node comprising clades I and J (BS: 100). Finally, 2 sequences were aligned within clade D and the last sequence was closely related to clade B, C and D. Regarding the sequences blasted for the partial 28S matrix, 2 sequences were extracted and mapped within clades E and G respectively.

Discussion

Morpho-molecular Classification of Living Nassellaria

In our phylogenetic classification the overall morphology of Nassellaria, rather than the initial spicular system, is the most accurate feature to differentiate clades at the Superfamily level (Supplementary Material Fig. S1). We could not find any pattern in the initial spicular system that enables to separate clades, suggesting that the complexity of the initial spicular system is not related to Nassellaria phylogeny (e.g., Acanthodesmoidea, Plagiacanthoidea). Yet, this morphological character has been used to discriminate families and higher taxonomical levels (Petrushevskaya 1971b). As well, the arches connecting these spicules were used in previous classifications and, in some cases, to discern at genus, and partly family levels (De Wever et al. 2001; Petrushevskaya 1971b). In addi-

Figure 3. Scanning Electron Microscopy (SEM) and/or Confocal Microscopy (CM) images of Nassellarian specimens used in this study for phylogenetic analysis or morphologically related to one of the morpho-molecular clades of Figure 1. Letters correspond to its phylogenetic clade in Figure 1. Scale bars = 50 μm. (A) Vil496: *Eucyrtidium acuminatum* (CM). (B) Osh128: *Polypleuris gigantea* (SEM). (C) Mge17-122: *Carpocanium* cf. *obliqua* (SEM). (D) Mge17-70: *Botryostrobus auritus* (SEM). (E1) Toy231: *Amphispyris costata* (SEM). (E2) Vil267: *Lophospyris* aff. *ivanovi* (SEM). (X1) Osh112: *Archipilium johannismonicae* (CM). (X2) Osh130: *Enneaphormis enneastrum* (SEM). (F) Mge17-94: *Eucecryphalus* aff. *cervus* (SEM). (G2) Osh50: *Pseudodictyophimus clevei* (CM). (G3) Vil269: *Acrobotrissa cribosa* (CM). (G4) Mge17-137: *Lipmanella* sp. (SEM). (G5) Ses60: *Peromelissa phalacra* (CM). (G6) Vil512: *Pseudocubus obeliscus* (CM). (H) Osh129: *Cycladophora cornuta* (CM). (I1 left) Osh184: *Lamprotripus hirundo* (SEM). (I1 right) Osh127: *Lamprotripus hirundo* (SEM). (I2) Vil225: *Pterocanium praetextum* (CM). (J1) Vil444: *Theocorythium dianae* (SEM).

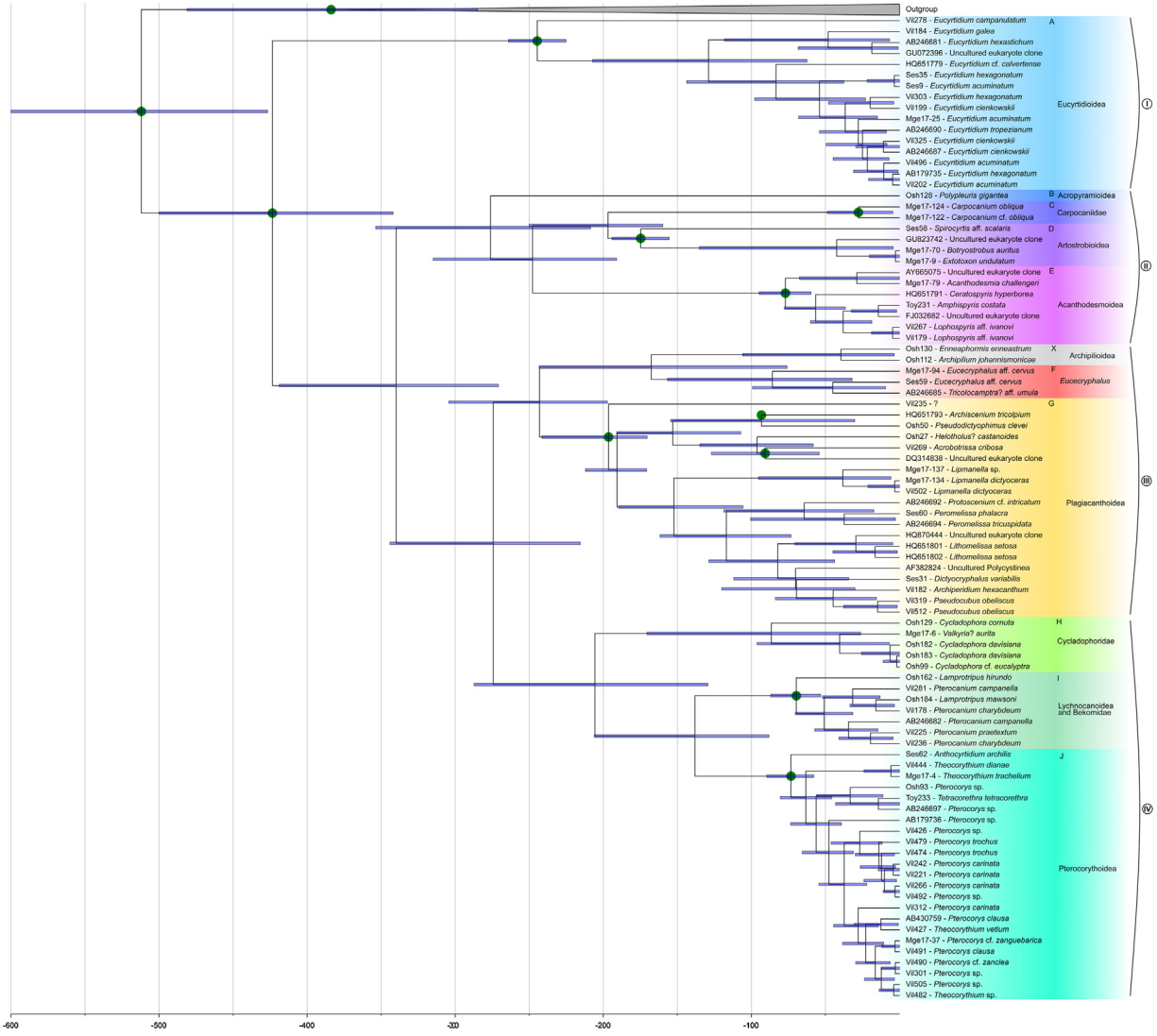

Figure 4. Time-calibrated tree (Molecular clock) of Nassellaria, based on alignment matrix used for phylogenetic analyses. Node divergences were estimated with a Bayesian relaxed clock model and the GTR + γ + I evolutionary model, implemented in the software package BEAST. Twelve different nodes were selected for the calibration (green dots). Blue bars indicate the 95% highest posterior density (HPD) intervals of the posterior probability distribution of node ages.

tion to our results, it has never been hypothesized the evolution of the initial spicular system complexity through the radiolarian fossil record. The use of the overall morphology in Nassellaria classification makes recognition of live cells easier under a light microscope facilitating morphology based ecological studies.

The extent Nassellaria included in our study can be divided in 11 morpho-molecular clades, grouped in four main evolutionary lineages based on phylogenetic clustering support, common morphological features and molecular dating: Eucyrtidioidea in lineage I; Acropyramioidea, Carpocaniidae, Artostrobioidea and Acanthodesmoidea in lineage II; Archipilioidea, Theopiliidae and Plagiacanthoidea in lineage III, and *Cycladophora*, Lychnocanoidea and Pterocorythoidea in lineage IV. The unified morpho-molecular framework here proposed reveals a partial agreement between the traditional taxonomy and the molecular classification. Such discrepancies have already been reported not only in other Radiolaria groups (Biard et al. 2015; Decelle et al. 2012b) but as well in other SAR taxa such as Foraminifera (Pawlowski and Holzmann 2002; Pawlowski et al. 2003), Phaeodaria (Nakamura et al. 2015) or Tintinnida (Bachy

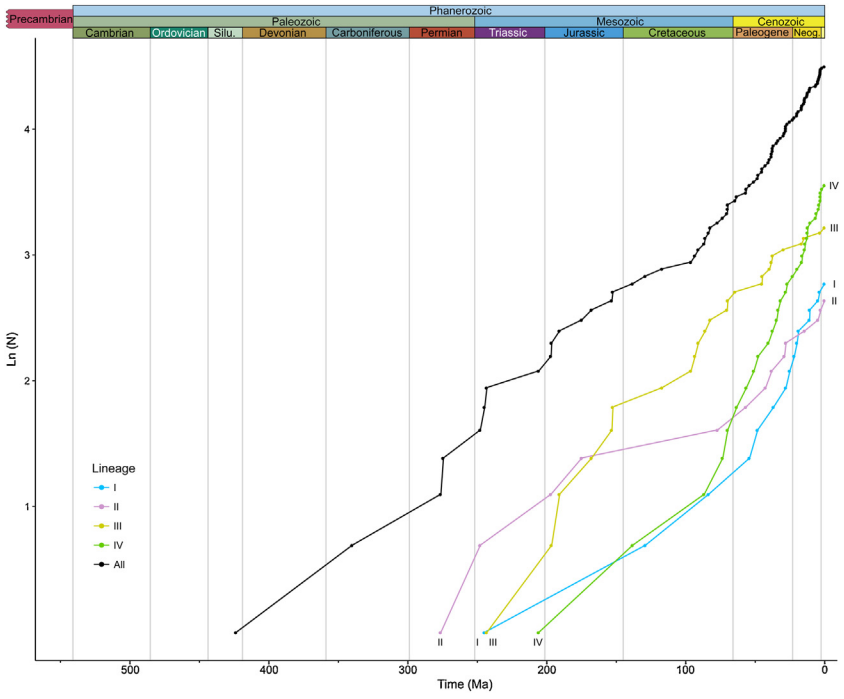

Figure 5. Lineages Through Time (LTT) analysis based on the molecular clock results for Nassellaria (removing the outgroup; in black), and of each lineage independently: lineage I (Blue), lineage II (purple), lineage III (yellow) and lineage IV (green). The y-axis represents the number of lineages (N) expressed in logarithmic (base e) scale (Ln(N)) and in the x-axis it is represented the time in million of years ago (Ma).

et al. 2012), being a common issue in protists classification (Caron 2013; Schlegel and Meisterfeld 2003).

Our revised morpho-molecular classification confirms the monophyly of the ancient Superfamilies Eucyrtidioidea and Acropyramioidea, represented by the clades A and B respectively, as well as the undetermined Family Carpocaniidae, and the Superfamilies Artostrobioidea and Acanthodesmoidea (clades C, D and E, respectively). The Superfamily Plagiacanthoidea is however paraphyletic, appearing in two different clades (X and G). Similarly, previously proposed families are scattered within clade G or even including the Superfamily Cannobotryoidea. Clade F and H both display an identical architecture of the initial spicular system, yet they are clustered based in the overall morphology in two different clades, the family here proposed as Theopiliidae (clade F) and *Cycladophora*-like specimens (clade H). As the genus *Eucecryphalus* (clade F) is the genus of the family Theopiliidae (see Matsuzaki et al. 2015), clade F holds the name Theopiliidae. Regarding clade H, a new family Cycladophoridae is established herein as defined in the taxonomic note. Regarding clades I and J, Matsuzaki et al. (2015) include them within the same Superfamily (Pterocorythoidea) due to the strong phylogenetic relationship reported by Krabberød et al. (2011). Yet due to the evolutionary patterns and the phylogenetic distance, these two clades should be considered as two different superfamilies, Pterocorythoidea and Lychnocanoidea (Lychnocanoidea Haeckel, 1882, sensu Kozur and Mostler 1984). In our study the undetermined family Bekomidae was scattered within clade I, showing no phylogenetic differences. Re-examination of the cephalic structure in *Lamprotripus* concludes the assignation of the genus to the Superfamily Lychnocanoidea, yet intergeneric morphological differences remain still elusive. Further molecular analyses must reveal these discrepancies between morphological and molecular classification.

Evolutionary History of Nassellaria

The morphological evolution of Nassellaria is marked by their dubious appearance in the fossil record, whether it happened with the primitive nassellarian forms (in the Upper Devonian) or with the first multi-segmented nassellarians (in the Early Triassic) (De Wever et al. 2001; Suzuki and Oba 2015). Our results showed that the first diversification of Nassellaria agrees in both time (~423

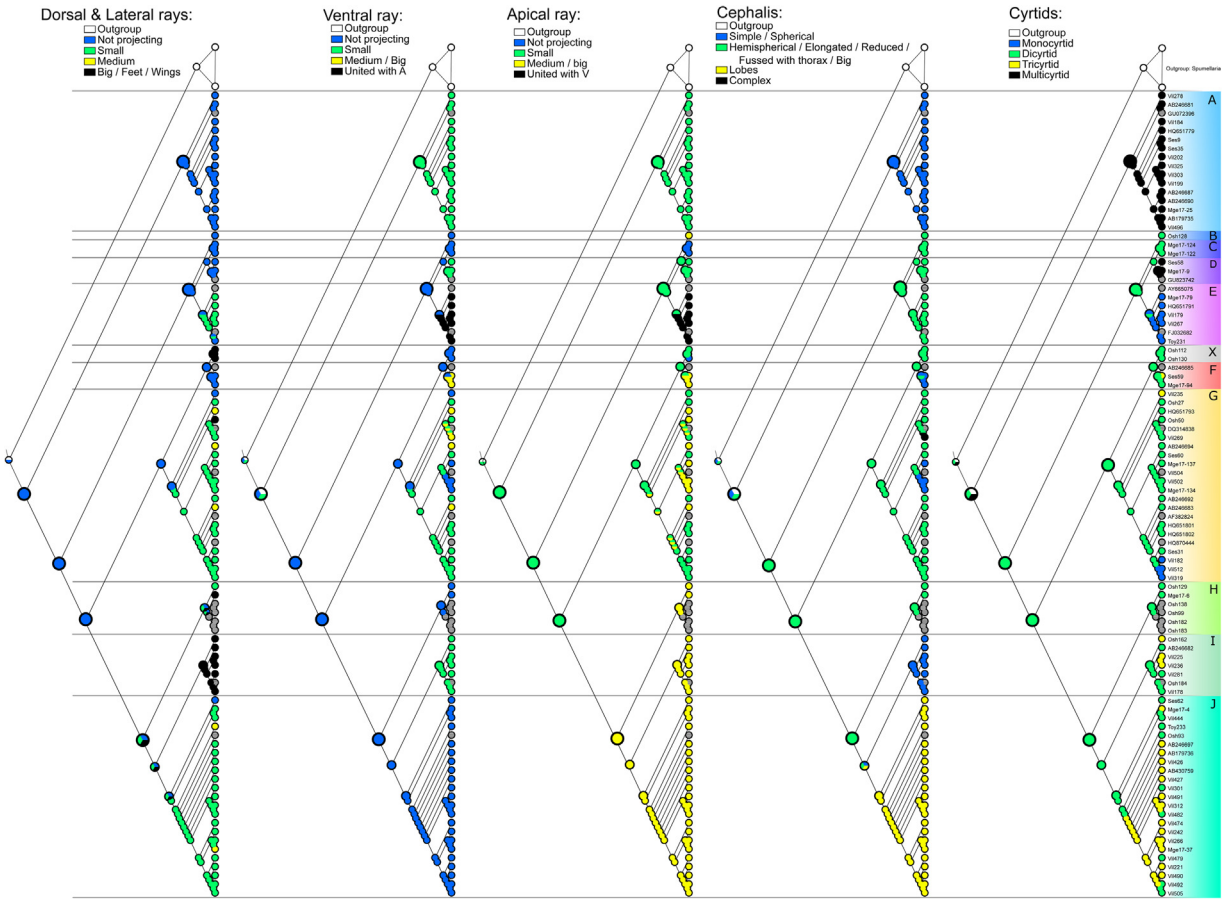

Figure 6. Parsimony Ancestral State Reconstruction analysis based in the resulting phylogenetic tree for the 5 characters chosen. Relevant nodes are increased for clarity.

Ma; 95% HPD: 500-342 Ma; Figs 4, 5) and reconstructed morphology (two- or multi-segmented last common ancestor) with the primitive nassellarians. Thus, the most likely scenario, proposed by Petrushevskaya (1971a) and continued by Cheng (1986), is where Nassellaria originated during the Devonian from primitive radiolarian forms and not during the Triassic. This hypothesis can explain the sudden appearance of forms in the Middle Triassic already pointed out by De Wever et al. (2003) and confirmed by our results.

The oldest known nassellarian like fossils are Popofskyellidae and Archocyrtiidae from the Devonian (Cheng 1986). The former family shares with lineage I a multisegmented nature of the skeleton whereas the Archocyrtiidae has a unique and large cephalic segment and three long feet, derived characteristics that can be found over lineages II, III and IV. Such similarities in the morphology and the accordance of the molecular clock in the branching times with the fossil record allow us to hypothesis these two families as possible ancestors of living Nassellarians; as already suggested by Cheng (1986). Thereafter, the evolutionary connection of Popofskyellidae and lineage I is debatable, due to a fragmented fossil record along the Permian (De Wever et al. 2003; Isakova and Nazarov 1986). Regarding lineage II, it is likely that diverged from Archocyrtiidae by reduction of the feet, though phylogenetic relationships within this lineage remain still unclear. A second morphological modification might have happened in the separation of the cephalis and thorax and the appearance of lineage IV (probable candidate is the Ultranaporidae). Therefore, Archocyrtiidae could be a direct ancestor of lineage III due the strong similarities within the members of this lineage and the Palaeozoic Archocyrtiidae.

Despite the early appearance of the Order Nassellaria, living nassellarian groups diversified ca. 250 Ma after the third, and biggest of all, mass extinction (Bambach et al. 2004; Sepkoski 1981). This bottle neck led to a rapid increase in the global marine diversity (Twitchett et al. 2004),

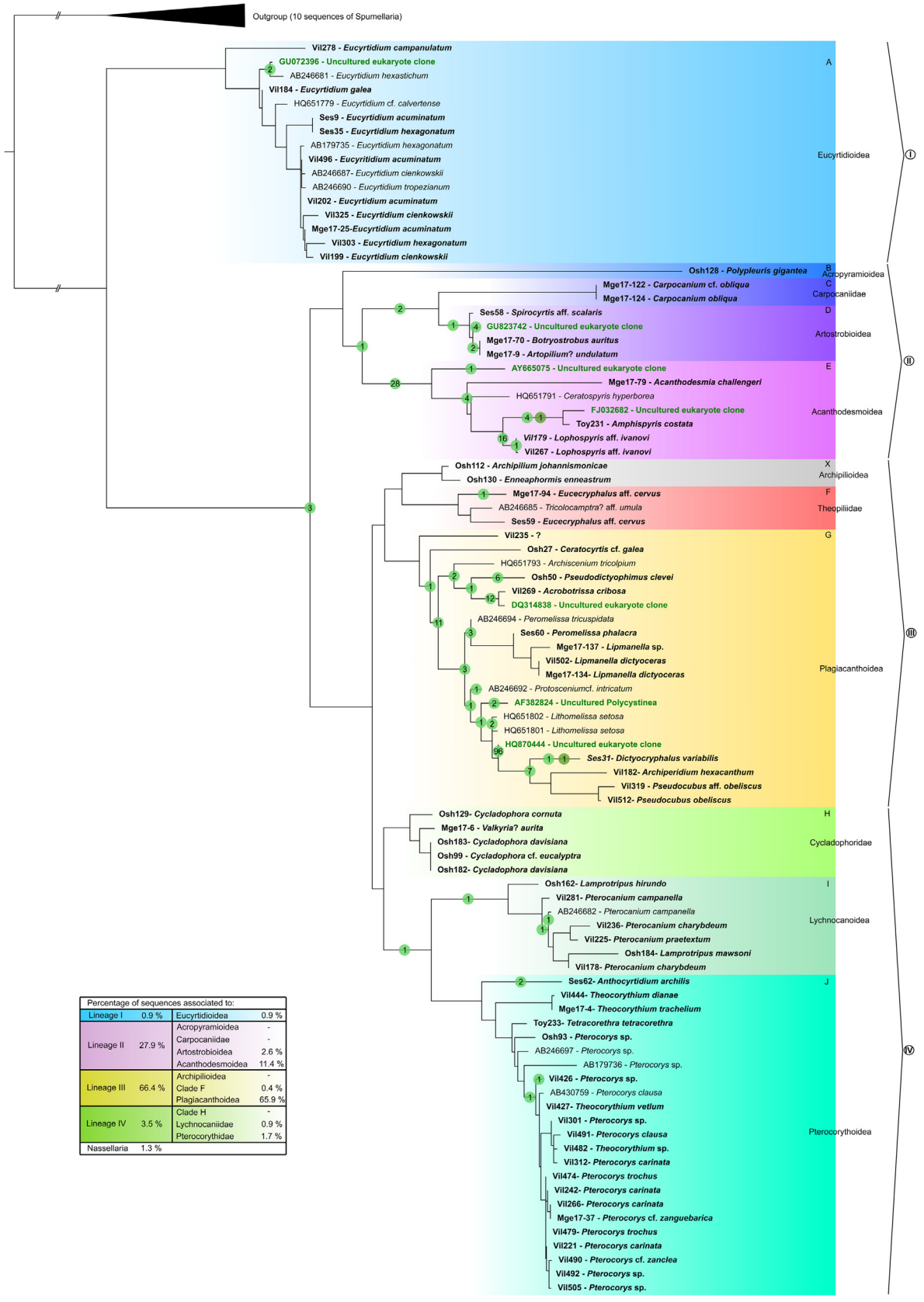

Percentage of sequences associated to:			
Lineage I	0.9 %	Eucyrtidioidea	0.9 %
Lineage II	27.9 %	Acropyramioidea	-
		Carpocaniidae	-
		Artostrobioidea	2.6 %
		Acanthodesmoidea	11.4 %
Lineage III	66.4 %	Archipilioidea	-
		Clade F	0.4 %
		Plagiacanthoidea	65.9 %
Lineage IV	3.5 %	Clade H	-
		Lychnocaniidae	0.9 %
		Pterocorythidae	1.7 %
Nassellaria	1.3 %		

where all the surviving and isolated populations followed different pathways; an expected process in the aftermath of an evolutionary crisis (Hull 2015; Twitchett and Barras 2004). The lineage of Acropyramioidea/Acanthodesmoidea (lineage II) splits apart into many different forms that will led to new families, lineages III and IV diverge from each other followed by a fast branching of the plagiacanthoids, while eucyrtidioids (lineage I) slowly diversifies. By the end of the Late Triassic-Early Jurassic, radiolarian fossil record reaches its highest diversity measures (De Wever et al. 2006). Along with Nassellaria, other groups of marine protists also diversified such as dinoflagellates (Fensome et al., 1996; Janouškovec et al., 2017) or even appeared like diatoms (Kooistra and Medlin 1996; Sims et al. 2006).

The second part of the Mesozoic is characterized by a global oceanic anoxic event happening at the end of the early Jurassic (Jenkyns 1998) and a widespread series of Oceanic Anoxic Events (known as OAEs) during the Cretaceous (Jenkyns 2010; Schalanger and Jenkyns 1976). These events have been proposed as the major responsible force for the appearance of planktic Foraminifera during the Jurassic (Hart et al. 2003), and for extinction-speciation processes in planktonic evolution during the Cretaceous, especially for Foraminifera and Radiolaria (Leckie et al. 2002). During the same period, we can find the rise of the Artostrobioidea, the divergence of the superfamilies Pterocorythoidea and Lychnocanoidea or the continuous diversification of the lineage III. After the OAEs and during the Early Cenozoic populations isolated from each other and probably thrived by the favourable conditions, start diversifying into the most recent families (Acanthodesmoidea, Theopiliidae, Cycladophoridae fam. nov., Lychnocanoidea, Pterocorythoidea and probably Archipilioidea). During the Cenozoic, other groups were also recovered from small populations linked to climate oscillations such as Foraminifera (Hallock et al. 1991) or calcareous Coccolithophores (Bown et al. 2004). Finally, during the late Cenozoic, the most recent family (Carpocaniidae) and groups (i.e., *Lipmanella* clade within Plagiacanthoidea) appear or diversify probably just before the opening of the Tasmanian gateway between Antarctica and Australia to form Antarctic Circumpolar Current.

Environmental Genetic Diversity of Nassellaria

Little is known about the diversity and ecology of contemporary Nassellaria. Despite recent studies using plankton net data publicly available (Boltovskoy et al. 2010; Boltovskoy and Correa 2016; Boltovskoy 2017), most of the knowledge on this taxa is inferred from their extensive fossil record worldwide (De Wever et al. 2001; Petrushevskaya 1971a). The present morpho-molecular framework proposes a morphological classification based on the overall structure, a feature easier to access compared to internal spicular structures, and therefore facilitating morphology-based ecological studies. Our framework also establishes a reference for sequences-based environmental diversity surveys and molecular ecology studies, allowing the accurate and fast taxonomic assignment of metabarcoding data.

Here we considered publicly available environmental sequences closely related to Nassellaria, from various environment (e.g. Edgcomb et al. 2011; Lie et al. 2014; Orsi et al. 2012) into our morpho-molecular data frame (Fig. 7). Most of environmental sequences clustered within the Superfamily Plagiacanthoidea, revealing an underrepresentation of this taxon in our study despite the number of sequences included (23%). This clade can be found at high relative abundances all year round (Ikenoue et al. 2015; Motoyama et al. 2005), in every latitude (Boltovskoy et al. 2010) and at every depth (Boltovskoy 2017). Most of the known plagiacantoid species are very small related to the average nassellarian size, so they could go through the plankton nets or be overlooked during isolation. Also, Acanthodesmoidea and Artostrobioidea are two clades highly represented in environmental sequences compared to the number of morphologically described sequences included in our study. The former superfamily is represented by sequences coming mainly from the subtropical and tropical South China Sea where Radiolaria are very abundant (Wu et al. 2014). The Artostrobioidea is mainly characterised by deep environmental sequences, an environment poorly represented in

Figure 7. Pplacer phylogenetic placement of 229 environmental sequences for the 18S rDNA gene and 2 environmental sequences for the 28S rDNA gene into a concatenated phylogenetic tree of Nassellaria (complete 18S + partial 28S rDNA genes). Numbers at nodes represent the amount of environmental sequences assigned to a branch or a node; in light green for the 18S rDNA gene and in dark green for the 28S rDNA gene.

our phylogenies mainly due to the difficulties in the DNA amplification of nassellarian specimens habiting the deep ocean. Likewise, the Superfamily Acropyramioidea, restricted to the deep ocean, is represented by only one sequence of the 28S rDNA gene. Therefore, due to the lack of 18S rDNA marker for this clade, it is likely that some of the sequences clustered within this lineage actually belong to the Acropyramioidea, since most of them come from deep environments (e.g., Kim et al. 2012; Lie et al. 2014; Xu et al. 2017). Increasing molecular coverage of the reference sequence database, through exploration of a variety of ecosystems, will be critical to properly decipher placement of environmental sequences. Our integrated approach enables providing a robust evolutionary history and classification of Nassellaria, and allows future ecological and diversity studies based in both a morphology or through a metabarcoding approach.

Taxonomic Notes

Following the molecular phylogenetic results, the definition of superfamilies is revised and a new family is established here following ICZN2000.

Superfamily **Eucyrtidioidea** Ehrenberg, 1846 sensu emend here by Suzuki.

Type genus. *Eucyrtidium* Ehrenberg, 1846 (type species: *Lithocampe acuminata* Ehrenberg).

Emended definition. A spherical cephalis with a sharply constricted basal aperture and many segmentations which are generally divided by inner rings. No feet.

Remarks. This Superfamily corresponds to clade A. Although many suggestions about the definition have been made so long (see Matsuzaki et al. 2015), these two points are only different points from other nassellarians.

Superfamily **Archipilioidea** Haeckel, 1882 stat. nov. by Sandín, Not and Suzuki.

Type genus. *Archipilium* Haeckel, 1882 (type species: *Archipilium orthopterum* Haeckel).

Definition. Practically single segment, although the upper and lower parts can be recognized by the position of *MB*. Initial spicular system is characterized by a very short *MB* (or missing) to form a three-pointed star rod system and a significant circular frame. Three feet or relevant structure is present.

Remarks. This corresponds with our Clade X. The figured specimens of the type species of *Archipilium* apparently lack a three-pointed star rod system and "a significant circular frame" (PR in Fig. S1). The intermediate form between *Archipilium* and *Enneaphormis* was described as "*Enneaphormis trippula*" by Renaudie and Lazarus (2016).

Family **Archipilidiae** Haeckel, 1882.

Type genus. *Archipilium* Haeckel, 1882 (type species: *Archipilium orthopterum* Haeckel).

Remarks. Here we include genera *Archibursa* Haeckel, 1882 (type species: *Archibursa tripodiscus* Haeckel), *Chitascenium* Sugiyama, 1994 (type species: *Chitascenium cranites* Sugiyama), and *Enneaphormis* Haeckel, 1882 (type species: *Sethophormis* (*Enneaphormis*) *rotula* Haeckel), because they have a three-pointed star rod system and a significant circular frame (PR).

Superfamily **Plagiacanthoidea** Hertwig, 1879 emended here by Sandín and Suzuki.

Type genus. *Plagiacantha* Claparede and Lachmann, 1859 (type species: *Acanthometra arachnoides* Claparède).

Emended definition. Test can be divided into upper and lower parts by the level of *MB* or the neck of test. Test is small, and the initial spicular system contains variable types of arches. By these arches, antecephalic lobe, eucephalic lobe and postcephalic lobes are formed. This Superfamily also includes nassellarians made of bony frame only.

Remarks. This definition includes both Plagiacanthoidea and Cannobotryoidea. The name "Plagiacanthoidea" has a priority to Cannobotryoidea.

Family **Cycladophoridae** fam. nov. Suzuki

Type genus. *Cycladophora* Ehrenberg, 1846 (type species: *Cycladophora davisiana* Ehrenberg)

Definition. Initial spicule with *A*-, *V*-, *D*- and two *L*-rods, and an *MB*. No *PR* and No tubular cephalis horn. Test robust, helmet-conical, consisting of two segments with or without frill-like fringe. Cephalis small, spherical, and pore-less or relict pores; distinctive from thorax; three wing-like rod or rims on upper thoracic wall.

Remarks. This new family is newly proposed to separate genus *Eucecryphalus*, the type genus of the family Theopiliidae, from *Cycladophora* which was used to belong to the Theopiliidae. More

study needs to determine differences between Cycladophoridae fam. nov. and Theopiliidae. The former's test is robust whereas the latter's one is fragile. Superfamily is not determined to Cycladophoridae because nothing is known about the phylogenetic relationship with the Mesozoic family Neosciadiocapsidae. Cycladophoridae fam. nov. differs from the Superfamily Lychnocanoidea in that the latter has three distinctive feet which are connected through thoracic rims from *A*-, *V*-, and two *L*-rods. Cycladophoraidae fam nov. is easily distinguished from the Superfamily Pterocorythoidea in having a pterocorythid cephalic structure with special lobes.

Methods

Sampling and single cell isolation: Plankton samples were collected off Sendai (38° 0′ 28.8″ N, 142° 0′ 28.8″ E), Sesoko (26° 48′ 43.2″ N, 73° 58′ 58.8″ E), the Southwest Islands, South of Japan (28° 14′ 49.2″ N, 129° 5′ 27.6″ E), in the bay of Villefranche-sur-Mer (43° 40′ 51.6″ N, 7° 19′ 40.8″ E) and in the west Mediterranean (MOOSE-GE cruise) by net tows, Vertical Multiple-opening Plankton Sampler (VMPS) or Bongo net (20–300 μm). More information on sampling methodology can be found in the RENKAN database (http://abims.sb-roscoff.fr/renkan). Targeted specimens were individually handpicked with Pasteur pipettes from the samples and transferred 3–4 times into 0.2 μm filtered seawater to allow self-cleaning from debris, particles attached to the cell or preys digestion. Images of live specimens were taken under an inverted microscope and thereafter transfer into 1.5 ml Eppendorf tubes containing 50 μl of molecular grade absolute ethanol and stored at −20 °C until DNA extraction.

Single cell morphological identification: Nassellaria specimens were identified at the species level, referring to pictures of holotypes and reliable specimens, through observation of live images and posterior analysis of the skeleton by scanning electron microscopy and/or confocal microscopy. At the species, genus and family levels, we respected the Articles 66 to 70 of "types in the genus group" in the International Code of Zoological Nomenclature 2000 (hereinafter ICZN 2000; http://www.iczn.org/iczn/index.jsp). The family level was decided by the similarity of the type genus of the family based on ICZN 2000. This procedure has the advantage to directly use the fossil taxonomy (Matsuzaki et al. 2015) and the taxonomic concept of superfamily (Matsuzaki et al. 2015; Suzuki and Not 2015) without ambiguity in the name used. Based on this rule, we updated the species name of specimens illustrated in previous studies and that are included in our phylogeny (see Supplementary Material Table S1 for taxonomic authority of specimens included in our study).

DNA extraction, amplification and sequencing: DNA was extracted using the MasterPure Complete DNA and RNA Purification Kit (Epicentre) following manufacturer's instructions. Once DNA was extracted and recovered, waste (i.e., pellet debris) from the extraction procedure were diluted in milliQ water to preserve skeletons and stored at −20 °C. Both 18S rDNA and pa rtial 28S rDNA genes (D1 and D2 regions) were amplified by Polymerase Chain Reaction (PCR) using Radiolaria and Nassellaria specific and general primers (Table 1). For further details about rDNA amplification see: https://www.protocols.io/view/single-cell-rdna-amplification-of-nassellaria-radi-t5req56. PCR amplicons were visualized on 1% agarose gel stained with ethidium bromide. Positive reactions were purified using the Nucleospin Gel and PCR Clean up kit (Macherey Nagel), following manufacturer's instructions and sent to Macrogen Europe for sequencing.

Phylogenetic analyses: After sequencing, forward and reverse sequences were checked and assembled using ChromasPro software version 2.1.4 (2017). Sequences were compared to reference database (GenBank) using the *BLAST search* tool integrated in ChromasPro to discriminate radiolarian sequences from possible contamination. Similar sequences identified in GenBank were retrieved and integrated in our databases. Two different datasets for each genetic marker (18S rDNA gene and partial 28S rDNA gene) were obtained and align separately using Muscle (Edgar 2004) implemented in SeaView version 4.6.1 (Gouy et al., 2010) and manually checked. For both genes, the 18S rDNA (61 taxa, 1890 positions) and the 28S rDNA (57 taxa, 700 positions), phylogenetic analyses were performed independently. The best nucleotide substitution model was chosen following the corrected Akaike Information Criterion (AICc) using the *modelTest* function implemented in the R (R Core Team 2014) package *phangorn* (Schliep, 2011). The obtained model (General Time Reversible with Gama distribution and proportion of Invariable sites, GTR + G + I) was applied to each data set in R upon the packages *APE* (Paradis et al. 2004) and *phangorn* (Schliep 2011). A Maximun Likelihood (ML) method (Felsenstein 1981) with 1000 replicates of bootstrap (Felsenstein 1985) was performed to infer phylogenies. Since the topology and bootstrap support within main clades of both markers agree, the 18S rDNA and the 28S rDNA were concatenated in order to improve phylogenetic resolution. A final data set containing 90 taxa and 2590 positions was used to infer phylogenies following the previous methodology. The best model obtained was GTR + G + I, with 4 intervals of the discrete gamma distribution, and a ML method with 100 000 bootstraps were performed. In parallel, a Bayesian analysis was performed using BEAST version 1.8.4 (Drummond et al. 2012) with the same model parameters over 10 million generations sampled every 1000 states, to check the consistency of the topology and to calculate posterior probabilities. Final tree was visualized and edited with FigTree version 1.4.3 (Rambaut 2016). All sequences obtained in this study and used for the phylogeny were submitted in GenBank under the accession numbers: MK396913–MK397005.

Molecular clock analyses: The resulting concatenated dataset of the 18S rDNA and the partial 28S rDNA used to infer phylogenies, was used for the molecular clock analyses following established protocols implemented in BEAST version 1.8.4 (Drummond et al. 2012). In order to avoid the assumption of substitution rates correlation between neighbour branches, a Bayesian uncorrelated relaxed clock method (Drummond et al. 2006) was performed to calculate the divergence times of Nassellaria with a relaxed lognormal distribution. GTR + G + I with estimated base frequencies and 4 gamma categories was chosen for the substitution model, according to previous analyses (see section above). Both Spumellaria (outgroup) and Nassellaria nodes were forced to be monophyletic according to bootstrap results in the phylogenetic analysis. According to software options, a speciation Yule process (Gernhard 2008, Yule 1925) with random starting tree was chosen as tree prior, since our analyses are beyond population level. Markov chains were run in three parallel replicates for 100 million generations sampled every 1000 states and operators were left as default. Different replicates were combined in LogCombiner ver-

Table 1. Primer sequences used for DNA amplification and sequencing.

Targeted gene	Primer	Specificity	Sequence 5′-3′	Direction	Tm °C	Reference
18S (1st part)	SA	Eukaryotic	AAC CTG GTT GAT CCT GCC AGT	Forward	56-60	Medlin et al., 1988
	18S NasIb R	Nassellaria	GAG ACT ACG ACG GTA TCT GAT C	Reverse	60	This study
	S879	Radiolaria	CCA ACT GTC CCT ATC AAT CAT	Reverse	56	Decelle et al., 2012b
	S32_TASN	Radiolaria	CCA GCT CCA ATA GCG TAT RC	Forward	52	Ishitani et al. 2012
18S (2nd part)	V9R	Eukaryotic	CCT TCY GCA GGT TCA CCT AC	Reverse	52	Romac (Unpub.)
	18S NassII F	Nassellaria	AGC ATG GAA TAA TAA CTG ATG A	Forward	57	This study
	18S NassII R	Nassellaria	CAC CAR TTC ATC CAA TCG GTA G	Reverse	57	This study
28S (D1 + D2)	28S Nas F	Nassellaria	AGT AAC GGC GAG TGA AGC	Forward	56	This study
	28S Nas R	Nassellaria	CCA ACA TAC DTG CTC TTG T	Reverse	56	This study
	28S Rad2	Radiolaria	TAA GCG GAG GAA AAG AAA	Forward	50	Ando et al., 2009
	ITSa3	Radiolaria	TCA CCA TCT TTC GGG TCC CAA CA	Reverse	50	Ando et al., 2009

Table 2. List of morphological characters (traits) and their states (1 to 4) used for the ancestral state reconstruction analysis.

		Traits				
		Number of segments	Complexity of cephalis	Apical ray	Ventral ray	Dorsal and lateral rays
State	1	Monocyrtid	Simple, Spherical	Not projecting the skeleton	Not projecting the skeleton	Not projecting the skeleton
	2	Dicyrtid	Hemispherical, elongated, Reduced, fussed with thorax	Small	Small	Small
	3	Tricyrtid	Lobes	Medium, big	Medium, big	Medium
	4	Multicyrtid	Complex	United with V	United with A	Big, foot, wings

sion 1.8.4 (Drummond et al. 2012) after removing the first 25% states. Twelve nodes were chosen to carry out this calibration (explained below from the oldest to the newest calibration age, and given the name of the node for the taxa they cover):

1. Root: The calibration for the root of the tree corresponds to the hypothesized last common ancestor between Nassellaria and Spumellaria (De Wever et al. 2001). A uniform distribution with a minimum bound of 200 million years ago (Ma) and a maximum of 600 Ma (U [200,600]) was set to allow uncertainty in the diversification of both groups and to establish a threshold restricting the range of solutions for the entire tree.
2. Spumellaria: The second node corresponds to the origin of Spumellaria, the outgroup of our phylogenetic analyses. The first spumellarians appear in the fossil record in the Lower Ordovician (ca. 477.7–470 Ma) with the genera *Antygopora* (Aitchison et al. 2017). Therefore, the node was normally distributed with a mean of 474 and a standard deviation of 50 to avoid uncertainty due to the low genetic diversity of the outgroup: N (474, 50).
3. Nassellaria: The first nassellarian-like fossil appear in the Devonian (ca. 419.2–358.9 Ma) with internal spicules typical from Nassellaria (Cheng 1986; Kiessling and Tragelehn 1994; Schwartzapfel and Holdsworth 1996). But it is not until the Early Triassic (ca. 250–240 Ma) that the first multisegmented nassellarians appeared in the fossil record (De Wever et al. 2003; Dumitrica 2017; Hori et al. 2011; Sugiyama 1992, 1997). Because it is unclear whether the first nassellarian-like fossils are true nassellarians, a uniform distribution with a maximum boundary of 500 and a minimum of 180 (U [180,500]) was chosen to allow uncertainty in the origin of living Nassellaria (Suzuki and Oba 2015).
4. Eucyrtidioidea N (246, 10): The first appearance of this family in the fossil record is with the genus *Triassocampe* (Sugiyama 1997) in the early Middle Triassic (Anisian: ca. 246.8–241.5). And there are continuous fossil record since the Carnian (ca. 237–228.5 Ma; as well Late Triassic) to present of the genus *Eucyrtidium* (De Wever et al. 2001, 2003; Petrushevskaya 1971a). Hence, the node was normally distributed with an average mean of 246 and a standard deviation of 10 (N (246, 10)).
5. Lophophaenidae N (191, 10): This family belongs to the Superfamily Plagiacanthoidea, and the genus *Thetisolata* in the Early Jurassic (Pliensbachian: ca. 191.4–183.7 Ma) is the oldest fossil record associated to this family (De Wever 1982).
6. Artostrobioidea N (182, 10): The genus *Artostrobium,* questionably assigned by Matsuoka (2004), is the oldest fossil for this family, and its first appearance in the fossil record is dated in the Early Jurassic (Toarcian: ca. 183.7–174.2 Ma) (Matsuoka 2004).
7. Sethoperidae N (180, 30): Like Lophophaenidae, this family also belongs to the Plagiacanthoidea, but its first appearance in the fossil record dates in the Middle Jurassic (Bajocian: ca. 170.3–168.3 Ma) with the genus *Turriseiffelus* (Dumitrica and Zügel 2003). However, the fossil record of this family seems to be patched, since the very first member associated to this family is restricted to a single stage in the Early Jurassic (genus *Carterwhalenia*, Pliensbachian: ca. 191.4–183.7) (O'Dogherty et al. 2009). Due to this uncertainty in the appearance of this family, we decided to increase the node prior standard deviation to 30 Ma.
8. Cannobotryoidea N (122, 20): Petrushevskaya (1971b) dated the first appearance of this family in the Cretaceous (ca. 145–66 Ma), and later the time frame was restricted to the Early Cretaceous (ca. 145–100 Ma) (De Wever et al. 2001, 2003). However, there is no consensus about whether the first morphologically similar genera (*Ectonocorys* or *Solenotryma*) to this group that appear in the fossil record really belong to it or not. Therefore, since no adequate evidence has been shown we slightly increase the standard deviation (sd: 20 Ma) for this node prior to allow uncertainty (Matsuzaki et al. 2015; O'Dogherty et al. 2009).
9. Acanthodesmoidea N (66, 10): The three families belonging to this superfamily (Acanthodesmiidae, Stephaniidae, Triospyrididae) have their first appearance in the fossil record in the Paleocene (ca. 66–56) (De Wever et al. 2001, 2003; Petrushevskaya 1971a), and the first genus described associated to this families corresponds to *Tholospyris* in the Early Paleocene (Kozlova 1983, 1999).
10. Bekomidae N (62, 10): The genus *Bekoma* (as representative of the family Bekomidae) has its first appearance in the Late Paleocene (ca. 66–56) (De Wever et al. 2001; Nishimura 1992).
11. Pterocorythidae N (57, 10): *Cryptocarpium* is the first, but doubted, representative of this family in the fossil record and it is dated in the Late Paleocene (ca. 66–56 Ma), followed by *Podocyrtis*, the first true representative, in the transition of the Eocene (ca. 56–33 Ma) (De Wever et al. 2001; Hollis 2006; Sanfilippo and Riedel 1992).
12. Carpocaniidae N (38, 10): The first representative of this family appears in the late Eocene (ca. 38–33.9 Ma) and correspond to the genus *Carpocanium* (De Wever et al. 2001; Kamikuri et al. 2012).

Post hoc analyses: In order to provide statistical support to our conclusions two different analyses were developed: a diversification of taxa over time (Lineages Through Time: LTT) and an ancestral state reconstruction. The former analysis was carried out with the *ltt.plot* function implemented in the package *APE* (Paradis et al. 2004) upon the tree obtained by the molecular dating analyses after removing the outgroup. The second analysis uses the resulting phylogenetic tree to infer the evolution of morphological characters. A numerical value was assigned to each state of a character trait, being 0 for the outgroup or the considered ancestral state, and 1 to 4 for Nassellaria or the presumed divergence state. In total 5 traits were consider (Table 2): the number of cyrtids/segments (1-monocyrtid, 2-dicyrtid, 3-tricyrtid, 4-multicyrtid), the complexity of the cephalis (1-simple/spherical, 2-hemispherical/elongated/reduced/fussed with thorax, 3-Lobes, 4-complex), the apical (A) ray, the ventral (V) ray (1-not projecting the skeleton, 2-small, 3-medium/big, 4-united with A/V) and the dorsal (D) and lateral rays (Lr and Ll) treated as one single character (D + Lr + Ll: 1-not projecting the skeleton, 2-small, 3-medium, 4-big/foot/wings). Once the character matrix was established a parsimony ancestral state reconstruction was performed to every character independently in Mesquite version 3.2 (Maddison and Maddison 2017).

Environmental sequences: Each nassellarian sequence of the 18S rDNA and partial 28S rDNA was compared with publicly available environmental sequences in GenBank (NCBI) using BLAST (as of December 2017); in order to estimate the environmental genetic diversity of Nassellaria and eventually to check the genetic coverage of our phylogenetic tree. Environmental sequences were placed in our reference phylogenetic tree using the pplacer software (Matsen et al. 2010). A RAxML (GTR + G + I) tree was built for the placement of the sequences

with a rapid bootstrap analysis and search for best-scoring ML tree and 1000 bootstraps.

Confocal (CM) and scanning electron microscopy (SEM): After DNA extraction, nassellarian skeletons were recovered from the eluted pellet and handpicked under binoculars or inverted microscope. After cleaning and preparing the skeletons (detailed protocol in dx.doi.org/10.17504/protocols.io.ug9etz6 for SEM and dx.doi.org/10.17504/protocols.io.t5qeq5w for CM; protocol for CM imaging extracted from dx.doi.org/10.17504/protocols.io.vuze6x6) images were taken with an inverted Confocal Microscopy (Leica TCS SP5 AOBS) and/or FEI Phenom table-top Scanning Electron Microscope (FEI technologies).

Acknowledgements

This work was supported by the IMPEKAB ANR15-CE02-0011 grant and the Brittany Region AREDC16 1520A01, the Japan Society for Promotion of Science KAKENHI Grand No. K16K0-74750 for N. Suzuki and "the Cooperative Research Project with the Japan Science and Technology Agency (JST) and Centre National de la Recherche Scientifique (CNRS, France) "Morpho-molecular Diversity Assessment of Ecologically, Evolutionary, and Geologically Relevant Marine Plankton (Radiolaria)". We are grateful to T/S Oshoro-maru (Hokkaido Univ.), T/S Toyoshio-maru (Hiroshima Univ.) and their directors, Susumu Ohtsuka (Hiroshima Univ.) and Atsushi Yamaguchi (Hokkaido Univ.), as well as Akihiro Tuji, Yasuhide Nakamura and Yoshiaki Aita for sampling in Oshoro-Maru. We would like to thank the MOOSE cruise and program for the opportunity of sampling and the facilities given onboard, as well as John Dolan for hosting us multiple times at the Laboratoire d'Océanographie of Villefranche sur Mer. We thank Sebastien Colin for the Confocal Microscope imaging. We are also very grateful to Peter Baumgartner for his valuable comments in geological events, and specially to Luis O'Dogherty, Spela Gorican and Taniel Danelian for sharing their knowledge in the fossil record and improving the calibration of the molecular clock.

Appendix A. Supplementary Data

Supplementary data associated with this article can be found, in the online version, at https://doi.org/10.1016/j.protis.2019.02.002.

References

Aitchison JC, Suzuki N, O'Dogherty L (2017) Inventory of Paleozoic radiolarian species (1880–2016). Geodiversitas **39**:533–637

Anderson OR (1993) The trophic role of planktonic foraminifera and radiolaria. Mar Microb Food Webs **7**:31–51

Anderson OR, Bennett P, Bryan M (1989) Experimental and observational studies of radiolarian physiological ecology: 3. Effects of temperature, salinity and light intensity on the growth and survival of Spongaster tetras tetras maintained in laboratory culture. Mar Micropaleontol **14**:275–282

Ando H, Kunitomo Y, Sarashina I, Iijima M, Endo K, Sashida K (2009) Intraspecific variations in the ITS region of Recent radiolarians. Earth Evol Sci **3**:37–44

Bachy C, Gómez F, López-García P, Dolan JR, Moreira D (2012) Molecular phylogeny of tintinnid ciliates (Tintinnida, Ciliophora). Protist **163**:873–887

Bambach RK, Knoll AH, Wang SC (2004) Origination, extinction, and mass depletions of marine diversity. Paleobiology **30**:522–542

Berney C, Pawlowski J (2006) A molecular time-scale for eukaryote evolution recalibrated with the continuous microfossil record. Proc R Soc B Biol Sci **273**:1867–1872

Biard T, Bigeard E, Audic S, Poulain J, Stemmann L, Not F (2017) Biogeography and diversity of Collodaria (Radiolaria) in the global ocean. ISME J **11**:1331–1344

Biard T, Pillet L, Decelle J, Poirier C, Suzuki N, Not F (2015) Towards an integrative morpho-molecular Classification of the Collodaria (Polycystinea, Radiolaria). Protist **166**:374–388

Boltovskoy D (2017) Vertical distribution patterns of Radiolaria Polycystina (Protista) in the World Ocean: living ranges, isothermal submersion and settling shells. J Plankton Res **39**:330–349

Boltovskoy D, Correa N (2016) Biogeography of Radiolaria Polycystina (Protista) in the World Ocean. Prog Oceanogr **149**:82–105

Boltovskoy D, Kling SA, Takahashi K, Bjørklund K (2010) World atlas of distribution of recent Polycystina (Radiolaria). Palaeontol Electron **13**:230

Bown PR, Lees JA, Young JR (2004) Calcareous Nannoplankton Evolution and Diversity Through Time. In Thierstein HR, Young JR (eds) Coccolithophores. Springer Berlin Heidelberg, pp 481–508

Burki F, Keeling PJ (2014) Rhizaria. Curr Biol **24**:103–107

Campbell AS (1954) Part D, Protista 3. Protozoa (Chiefly Radiolaria and Tintinnina). In Moore RC (ed) Treatise on Invertebrate Paleontology. Univ Kansans Press, Lawrence, KS,

Cardinal S, Danforth BN (2013) Bees diversified in the age of eudicots. Proc R Soc B Biol Sci **280**:20122686

Caron DA (2013) Towards a molecular taxonomy for protists: Benefits, risks, and applications in plankton ecology. J Eukaryot Microbiol **60**:407–413

Cheng Y-N (1986) Taxonomic studies on Upper Paleozoic Radiolaria. Spec Publ 1, Natl Mus Nat Sci Taiwan. 311 p.

Claparede E, Lachmann J (1859) Les infusoires et les Rhizopodes. Mem l'institut Natl Genev. p. 261–482

De Wever P (1982) Nassellaria (Radiolaires Polycystines) du Lias de Turquie. Rev Micropaléontologie **244**:189–232

De Wever P, O'Dogherty L, Goričan Š (2006) The plankton turnover at the Permo-Triassic boundary, emphasis on radiolarians. Eclogae geol Helv **99**:S49–S62

De Wever P, Dumitrica P, Caulet JP, Nigrini C, Caridroit M (2001) Radiolarians in the Sedimentary Record. Gordon & Breach Science Publishers, Amsterdam, 533 p

De Wever P, O'Dogherty L, Caridroit M, Dumitrica P, Guex J, Nigrini C, Caulet JP (2003) Diversity of radiolarian families through time. Bull Soc Geol Fr **174**:453–469

Decelle J, Colin S, Foster RA (2015) Photosymbiosis in Marine Planktonic Protists. In Ohtsuka S, Suzaki T, Horiguchi T, Suzuki N, Not F (eds) Marine Protists. Springer, Tokyo, pp 465–500

Decelle J, Suzuki N, Mahé F, De Vargas C, Not F (2012b) Molecular phylogeny and morphological evolution of the Acantharia (Radiolaria). Protist **163**:435–450

Decelle J, Martin P, Paborstava K, Pond DW, Tarling G, Mahé F, De Vargas C, Lampitt R, Not F (2013) Diversity, ecology and biogeochemistry of cyst-forming Acantharia (Radiolaria) in the Oceans. PLoS ONE **8(1)**:e53598

Decelle J, Probert I, Bittner L, Desdevises Y, Colin S, de Vargas C, Galí M, Simó R, Not F (2012a) An original mode of symbiosis in open ocean plankton. Proc Natl Acad Sci USA **109**:18000–18005

Douzery EJP, Snell EA, Bapteste E, Delsuc F, Philippe H (2004) The timing of eukaryotic evolution: Does a relaxed molecular clock reconcile proteins and fossils? Proc Natl Acad Sci USA **101**:15386–15391

Drummond AJ, Ho SYW, Phillips MJ, Rambaut A (2006) Relaxed phylogenetics and dating with confidence. PLoS Biol **4**:699–710

Drummond AJ, Suchard MA, Xie D, Rambaut A (2012) Bayesian phylogenetics with BEAUti and the BEAST 1. 7. Mol Biol Evol **29**:1969–1973

Dumitrica P (2017) On the status of the Triassic radiolarian family Hexapylomellidae Kozur and Mostler: Taxonomic consequences. Rev Micropaléontol **60**:33–85, http://dx.doi.org/10.1016/j.revmic.2016.09.003

Dumitrica P, Zügel P (2003) Lower Tithonian mono- and dicyrtid Nassellaria (Radiolaria) from the Solnhofen area (southern Germany). Geodiversitas **25**:72

Edgar RC (2004) MUSCLE: multiple sequence alignment with high accuracy and high throughput. Nucleic Acids Res **32**:1792–1797

Edgcomb V, Orsi W, Bunge J, Jeon S, Christen R, Leslin C, Holder M, Taylor G, Suarez P, Varela R, Epstein S (2011) Protistan microbial observatory in the Cariaco Basin, Caribbean. I. Pyrosequencing vs Sanger insights into species richness. ISME J **5**:1344–1356

Ehrenberg CG (1846) Über eine halibiolithische, von Herrn R Schomburgk entdeckte, vorherrschend aus mikroskopischen Polycystinen gebildete, Gebirgsmasse von Barbados. Ber Königl Preuß Akad Wiss Berlin **1846**:382–385

Eme L, Sharpe SC, Brown MW, Roger AJ (2014) On the age of eukaryotes: Evaluating evidence from fossils and molecular clocks. Cold Spring Harb Perspect Biol **6**:a016139

Felsenstein J (1981) Evolutionary trees from DNA sequences: A maximum likelihood approach. J Mol Evol **17**:368–376

Felsenstein J (1985) Phylogenies and the comparative method. Am Nat **125**:1–15

Fensome RA, MacRae RA, Moldowan JM, Taylor FJR, Williams GL (1996) The early Mesozoic radiation of dinoflagellates. Paleontol Soc **22**:329–338

Gernhard T (2008) The conditioned reconstructed process. J Theor Biol **253**:769–778

Giles S, Xu G, Near TJ, Friedman M (2017) Early members of 'living fossil' lineage imply later origin of modern ray-finned fishes. Nature **549**:265–268

Gouy M, Guindon S, Gascuel O (2010) SeaView Version 4: A multiplatform graphical user interface for sequence alignment and phylogenetic tree building. Mol Biol Evol **27**:221–224

Haeckel E (1882) Entwurf eines Radiolarien-Systems auf Grund von Studien der Challenger-Radiolarien. Jenaische Zeit Naturwiss **15**:418–472

Hallock P, Premoli Silva I, Boersma A (1991) Similarities between planktonic and larger foraminiferal evolutionary trends through Paleogene paleoceanographic changes. Palaeogeogr Palaeoclimatol Palaeoecol **83**:49–64

Hart MB, Hylton MD, Oxford MJ, Price GD, Hudson W, Smart CW (2003) The search for the origin of the planktic Foraminifera. J Geol Soc London **160**:341–343

Hertwig R (1879) Der Organismus der Radiolarien. Gustav Fischer, Jena, 149 p.

Hollis CJ (2006) Radiolarian faunal turnover through the Paleocene-Eocene transition, Mead Stream, New Zealand. Eclogae Geol Helv **99**:79–100

Hori RS, Yamakita S, Ikehara M, Kodama K, Aita Y, Sakai T, Takemura A, Kamata Y, Suzuki N, Takahashi S, Spörli KB, Grant-Mackie JA (2011) Early Triassic (Induan) Radiolaria and carbon-isotope ratios of a deep-sea sequence from Waiheke Island, North Island, New Zealand. Palaeoworld **20**:166–178

Hull P (2015) Life in the aftermath of mass extinctions. Curr Biol **25**:R941–R952

Ikenoue T, Bjørklund KR, Kruglikova SB, Onodera J, Kimoto K, Harada N (2015) Flux variations and vertical distributions of siliceous Rhizaria (Radiolaria and Phaeodaria) in the western Arctic Ocean: Indices of environmental changes. Biogeosciences **12**:2019–2046

Isakova TN, Nazarov BB (1986), Late Carboniferous – Early Permian stratigraphy and microfauna of Southern Urals. Tr. GIN, no. 402, 1–183 (in Russian with English abstract)

Janouškovec J, Gavelis GS, Burki F, Dinh D, Bachvaroff TR, Gornik SG, Bright KJ, Imanian B, Strom SL, Delwiche CF, Waller RF, Fensome RA, Leander BS, Rohwer FL, Saldarriaga JF (2017) Major transitions in dinoflagellate evolution

unveiled by phylotranscriptomics. Proc Natl Acad Sci USA **114**:E171–E180

Jenkyns HC (1998) The early Toarcian anoxic event: Stratigraphic, sedimentary, and geochemical evidence. Am J Sci **288**:101–151

Jenkyns HC (2010) Geochemistry of oceanic anoxic events. Geochem Geophys Geosystems **11**:Q03004

Kamikuri S-I, Moore TC, Ogane K, Suzuki N, Pälike H, Nishi H (2012) Early Eocene to early Miocene radiolarian biostratigraphy for the low-latitude Pacific Ocean. Stratigraphy **9**:77–108

Kiessling W, Tragelehn H (1994) Devonian radiolarian faunas of conodont-dated localities in the Frankenwald (northern Bavaria, Germany). Abh Geol Bundesanst Win **50**:219–225

Kim DY, Countway PD, Yamashita W, Caron DA (2012) A combined sequence-based and fragment-based characterization of microbial eukaryote assemblages provides taxonomic context for the Terminal Restriction Fragment Length Polymorphism (T-RFLP) method. J Microbiol Methods **91**:527–536

Kooistra WHCF, Medlin KL (1996) Evolution of the Diatoms (Bacillariophyta). Mol Phylogenet Evol **6**:391–407

Kozlova GE (1983) Radiolyarievye kompleksy boreal'nogo nizhnego paleotsenaRadiolyrii Paleogena boreal'noy oblasti Roccii, In Rol' Mikrofauny v Izutsenii Osadotsnykh Tolshsh Kontinentov i Morey. VNIGRI, Leningrad. p. 88–112

Kozlova GE (1999) Radiolarii paleogene boreal'noi oblasti Rossii. Practicheskoe rykovodstvo po microfayne Rossii. 9. VNIGRI Publishers, Sankt-Peterburg, 323 p (In Russian)

Kozur H, Mostler H (1984) Obzor sistematiki triasovykh radiolyariy. In Petrushevskaya MG, Stepanyants SD (eds) Morfologiya, Ekologiya i Evolyutsiya Radiolyariy. Nauka, Leningrad, pp 114–123 (in Russian with German abstract)

Krabberød AK, Brate J, Dolven JK, Ose RF, Klaveness D, Kristensen T, Bjørklund KR, Shalchian-Tabrizi K (2011) Radiolaria divided into Polycystina and Spasmaria in combined 18S and 28S rDNA phylogeny. PLoS ONE **6(8)**:e23526

Kunitomo Y, Sarashina I, Iijima M, Endo K, Sashida K (2006) Molecular phylogeny of acantharian and polycystine radiolarians based on ribosomal DNA sequences, and some comparisons with data from the fossil record. Europ J Protistol **42**:143–153

Leckie RM, Bralower TJ, Cashman R (2002) Oceanic anoxic events and plankton evolution: Biotic response to tectonic forcing during the mid-Cretaceous. Paleoceanography **17**, 13-1–13-29

Lewitus E, Bittner L, Malviya S, Bowler C, Morlon H (2018) Clade-specific diversification dynamics of marine diatoms since the Jurassic. Nat Ecol Evol **2**:1715–1723

Lie AAY, Liu Z, Hu SK, Jones AC, Kim DY, Countway PD, Amaral-Zettler LA, Cary SC, Sherr EB, Sherr BF, Gast RJ, Caron DA (2014) Investigating microbial eukaryotic diversity from a global census: Insights from a comparison of pyrotag and full-length sequences of 18S rRNA genes. Appl Environ Microbiol **80**:4363–4373

Maddison DR, Maddison WP (2017) Mesquite: A Modular System for Evolutionary Analysis. Version 3.2. https://www.mesquiteproject.org/

Matsen FA, Kodner RB, Armbrust EV (2010) pplacer: linear time maximum-likelihood and Bayesian phylogenetic placement of sequences onto a fixed reference tree. BMC Bioinformatics **11**:538

Matsuoka A (2004) Toarcian (Early Jurassic) radiolarian fauna from the Nanjo Massif in Mino terrane, central Japan. News Osaka Micropaleontologists (NOM), Spec **13**:69–87

Matsuzaki KM, Suzuki N, Nishi H (2015) Middle to Upper Pleistocene polycystine radiolarians from Hole 902-C9001C, northwestern Pacific. Paleontol Res **19(Supp)**:1–77

Medlin L, Elwood HJ, Stickel S, Sogin ML (1988) The characterization of enzymatically amplified eukaryotic 16S-like rRNA-coding regions. Gene **71**:491–499

Miller AK, Kerr AM, Paulay G, Reich M, Wilson NG, Carvajal JI, Rouse GW (2017) Molecular phylogeny of extant Holothuroidea (Echinodermata). Mol Phylogenet Evol **111**:110–131

Motoyama I, Ota M, Kokushou T, Tanaka Y (2005) Seasonal changes in fluxes and assemblages of radiolarians collected by sediment trap experiments in the northwestern Pacific: a family-level analysis. J Geol Soc Japan **111**:404–416

Nakamura Y, Imai I, Yamaguchi A, Tuji A, Not F, Suzuki N (2015) Molecular phylogeny of the widely distributed marine protists, Phaeodaria (Rhizaria, Cercozoa). Protist **166**:363–373

Nishimura A (1992) Paleocene radiolarian biostratigraphy in the Northwest Atlantic at Site 384, Leg 43, of the Deep Sea Drilling Project. Micropaleontology **38**:317–362

Nitsche F, Thomsen HA, Richter DJ (2016) Bridging the gap between morphological species and molecular barcodes-exemplified by loricate choanoflagellates. Europ J Protistol **57**:26–37

O'Dogherty L (1994) Biochronology and paleontology of Mid-Cretaceous radiolarians from Northern Apennines (Italy) and Betic Cordillera (Spain). Mém Géol (Lausanne) **21**: 1–415

O'Dogherty L, Carter ES, Dumitrica P, Goriččan Š, Wever P De, Bandini AN, Baumgartner PO, Matsuoka A (2009) Catalogue of Mesozoic Radiolarian Genera. Part 2: Jurassic-Cretaceous Catalogue of Mesozoic radiolarian genera. Geodiversitas **31**:271–356

Orsi W, Song YC, Hallam S, Edgcomb V (2012) Effect of oxygen minimum zone formation on communities of marine protists. ISME J **6**:1586–1601

Paradis E, Claude J, Strimmer K (2004) APE: Analyses of phylogenetics and evolution in R language. Bioinformatics **20**:289–290

Pawlowski J, Holzmann M (2002) Molecular phylogeny of Foraminifera – A review. Europ J Protistol **38**:1–10

Pawlowski J, Holzmann M, Berney C, Fahrni J, Gooday AJ, Cedhagen T, Habura A, Bowser SS (2003) The evolution of early Foraminifera. Proc Natl Acad Sci USA **100**:11494–11498

Petrushevskaya MG (1971a) Radiolarians of the World Ocean. Acad Sci USSR Inst Zool :393

Petrushevskaya MG (1971b) On the Natural System of Polycystine Radiolaria. In Proc 2nd Plankton Conf : pp 981–992

Petrushevskaya MG (1981) Nassellarian Radiolarians from the World Oceans. Zool Institute Acad Sci USSR. Nauk Leningr Otd Leningrad, 405 p (in Russian)

Probert I, Siano R, Poirier C, Decelle J, Biard T, Tuji A, Suzuki N, Not F (2014) *Brandtodinium* Gen. Nov. and B. *Nutricula* Comb. Nov. (Dinophyceae), A dinoflagellate commonly found in symbiosis with polycystine radiolarians. J Phycol **50**:388–399

R Core Team (2014) R: A Language and Environment for Statistical Computing., http://dx.doi.org/10.1007/978-3-540-74686-7

Rambaut A (2016) FigTree version 1.4.3. http://tree.bio.ed.ac.uk/software/figtree/

Renaudie J, Lazarus DB (2016) New species of Neogene radiolarians from the Southern Ocean –part IV. J. Micropalaeontol **35**:26–53

Riedel WR (1967) Some new families of Radiolaria. Proc Geol Soc London **1640**:148–149

Sanfilippo A, Riedel WR (1992) the origin and evolution of Pterocorythidae (Radiolaria) – a Cenozoic phylogenetic study. Micropaleontology **38**:1–36

Schalanger SO, Jenkyns HC (1976) Cretaceous oceanic anoxic events: causes and consequences. Geol Mijnb **55**:179–184

Schlegel M, Meisterfeld R (2003) The species problem in protozoa revisited. Europ J Protistol **39**:349–355

Schliep KP (2011) phangorn: Phylogenetic analysis in R. Bioinformatics **27**:592–593

Schwartzapfel JA, Holdsworth B (1996) Upper Devonian and Mississippian radiolarian zonation and biostratigraphy of the Woodford, Sycamore, Caney and Goddard Formation, Oklahoma. Cushman Found. Foraminifer Res Spec Publ **33**:1–275

Sepkoski JJ (1981) A factor analytic description of the Phanerozoic marine fossil record. Paleobiology **7**:36–53

Sims PA, Mann DG, Medlin LK (2006) Evolution of the diatoms: insights from fossil, biological and molecular data. Phycologia **45**:361–402

Sugiyama K (1992) Lower and Middle Triassic Radiolarians from Mt. Kinkazan Gifu Prefecture, central Japan. Trans Proc Palaeont Soc Japan **167**:1180–1223

Sugiyama K (1994) Lower Miocene new nassellarians (Radiolaria) from the Toyohama Formation Morozaki Group, central Japan. Bull Mizunami Foss Museum (Mizunami-shi Kadeki Hakubutsukan Kenkyu Hokoku) **21**:1–11

Sugiyama K (1997) Triassic and Lower Jurassic radiolarian biostratigraphy in the siliceous claystone and bedded chert units of the southeasern Mino Terrane, Central Japan. Bull Mizunami Foss Mus **24**:79–193

Sugiyama K, Hori RS, Kusunoki Y, Matsuoka A (2008) Pseudopodial features and feeding behavior of living nassellarians *Eucyrtidium hexagonatum* Haeckel, *Pterocorys zancleus* (Müler) and *Dictyocodon prometheus* Haeckel. Paleontol Res **12**:209–222

Suzuki N, Not F (2015) Biology and Ecology of Radiolaria. In Ohtsuka S, Suzaki T, Horiguchi T, Suzuki N (eds) Marine Protists. Diversity and Dynamics. Springer, Tokyo, pp 179–222

Suzuki N, Oba M (2015) Oldest Fossil Records of Marine Protists and the Geologic History Toward the Establishment of the Modern-Type Marine Protist World. In Ohtsuka S, Suzaki T, Horiguchi T, Suzuki N (eds) Marine Protists. Diversity and Dynamics. Springer, Tokyo, pp 359–394

Twitchett RJ, Barras CG (2004) Trace fossils in the aftermath of mass extinction events. Geol Soc London Spec Publ **228**:397–418

Twitchett RJ, Krystyn L, Baud A, Wheeley JR, Richoz S (2004) Rapid marine recovery after the end-Permian mass-extinction event in the absence of marine anoxia. Geology **32**:805–808, http://dx.doi.org/10.1130/G20585.1

Wu W, Huang B, Liao Y, Sun P (2014) Picoeukaryotic diversity and distribution in the subtropical-tropical South China Sea. FEMS Microbiol Ecol **89**:563–579

Xu D, Jiao N, Ren R, Warren A (2017) Distribution and diversity of microbial eukaryotes in bathypelagic waters of the South China Sea. J Eukaryot Microbiol **64**:370–382

Yuasa T, Dolven JK, Bjørklund KR, Mayama S, Takahashi O (2009) Molecular phylogenetic position of *Hexacontium pachydermum* Jørgensen (Radiolaria). Mar Micropaleontol **73**:129–134

Yule GU (1925) A mathematical theory of evolution based on the conclusions of Dr. J. C. Willis. F.R.S. Philos Trans R Soc Lond B Biol Sci **213**:21–87

Zhang L, Suzuki N, Yasuhide N, Tuji A (2018) Modern shallow water radiolarians with photosynthetic microbiota in the western North Pacific. Mar Micropaleontol **139**:1–27